

Limiting Conductivities of Univalent Cations and the Chloride Ion in H₂O and D₂O Under Hydrothermal Conditions

J. Plumridge · H. Arcis · P. R. Tremaine

Received: 15 March 2014 / Accepted: 9 December 2014 / Published online: 20 January 2015
© Springer Science+Business Media New York 2015

Abstract Frequency-dependent electrical conductivities of aqueous sodium chloride, potassium chloride, cesium chloride, potassium iodide and cesium iodide have been measured in both H₂O and D₂O between $T = 298$ and 598 K at $p \sim 20$ MPa at a ionic strength of $\sim 10^{-3}$ mol·kg⁻¹ using a high-precision flow-through AC electrical conductance instrument. Experimental values for the molar conductivity, Λ , of each electrolyte were used to calculate their molar conductivities at infinite dilution, Λ° , with the Fuoss–Hsia–Fernández-Prini conductivity model. Single-ion limiting conductivities for the chloride ion in H₂O, $\lambda^\circ(\text{Cl}^-)$, were derived from Λ° by extrapolating literature values for the transference number of Cl⁻, $t^\circ(\text{Cl}^-)$, in aqueous solutions of KCl and NaCl from ~ 400 and ~ 390 K up to the experimental conditions. Values for $\lambda^\circ(\text{Cl}^-)$ in D₂O were determined from literature values of $t^\circ(\text{Cl}^-)$ for KCl in D₂O near ambient conditions, assuming the same temperature dependence as in H₂O. The results were used to calculate values for the single ion limiting conductivities $\lambda^\circ(\text{Na}^+)$, $\lambda^\circ(\text{K}^+)$, $\lambda^\circ(\text{Cs}^+)$, $\lambda^\circ(\text{Cl}^-)$, and $\lambda^\circ(\text{I}^-)$ in both light and heavy water. The values of λ° in D₂O are the first to be reported at temperatures above 338 K. The temperature dependence of the isotopic Walden product ratio, $(\lambda^\circ\eta)_{\text{D}_2\text{O}}/(\lambda^\circ\eta)_{\text{H}_2\text{O}}$, indicates that differences in the hydration of Cl⁻, K⁺ and Cs⁺ ions between light and heavy water at ambient conditions associated with hydrogen-bonding, the so-called “structure breaking” effects, largely disappear at temperatures above ~ 400 K. The value of $(\lambda^\circ\eta)_{\text{D}_2\text{O}}/(\lambda^\circ\eta)_{\text{H}_2\text{O}}$ for the “structure making” ion Na⁺ rises from 0.98 at 298.15 K to $\sim 1.04 \pm 0.02$ at temperatures above ~ 375 K and remains approximately constant up to 600 K.

Electronic supplementary material The online version of this article (doi:10.1007/s10953-014-0281-1) contains supplementary material, which is available to authorized users.

J. Plumridge · H. Arcis · P. R. Tremaine (✉)
Department of Chemistry, University of Guelph, Guelph, ON N1G 2W1, Canada
e-mail: tremaine@uoguelph.ca

H. Arcis
e-mail: harcis@uoguelph.ca

Keywords Molar conductivities · Alkali metal cations · Aqueous electrolytes · Hydrothermal solutions · Ionic hydration · Deuterium isotope effects

1 Introduction

Ionic conductivity measurements have played a pivotal role in investigations aimed at understanding and quantifying ionic hydration effects, ion association, and acid–base ionization in high-temperature water [1–4]. The pioneering studies by Noyes [5–8], Franck [9], Marshall [10, 11] and others have been reviewed [4, 12]. Briefly, these measurements yielded ionization constants, association constants and transport properties of simple anions and cations up to temperatures as high as 800 °C and pressures up to 400 MPa. Such measurements yield limiting equivalent conductivities for electrically neutral salts, $\Lambda^\circ(\text{M}^+\text{X}^-)$. In order to determine the contribution of individual ions, an experimental value for the transference number must be used to derive the limiting equivalent conductivity of one ion, usually $\lambda^\circ(\text{Cl}^-)$. In a seminal paper, Marshall [13, 14] reported a reduced state relationship to predict limiting conductivities for simple mono- and divalent anions and cations from 273 to 1,073 K and up to 400 MPa, based on the limiting conductance data available at that time, largely from his own work. This calculation was based on values of $\lambda^\circ(\text{Cl}^-)$ obtained by extrapolating Smith and Dismukes' values [15] for the transference number of the chloride ion in NaCl(aq) which extended only up to 398 K.

Recent developments in the design and construction of static high temperature cells [16] and the introduction of high precision flow cells by Bianchi et al. [17], Wood and his co-workers [18–20] and Ho et al. [21–23] have yielded significant improvements in the speed and accuracy of conductivity measurements for very dilute solutions in the range 323–673 K at pressures up to 40 MPa. Limiting conductivities from measurements in high-precision cells have now been reported for the salts of the univalent ions H^+ , Li^+ , Na^+ , K^+ , Cs^+ , Cl^- , Br^- , and OH^- in light water over this range, as cited in the review by Corti et al. [2]. More recent measurements have yielded values of λ° for Li^+ , Na^+ , K^+ , Ca^{2+} , HSO_4^- , SO_4^{2-} , acetate and their ion pairs [20, 24–27]. These are all based on Marshall's [13, 14] values for $\lambda^\circ(\text{Cl}^-)$. In 2012, Zimmerman et al. [28] reported a correlation of critically reviewed modern values for $\Lambda^\circ(\text{NaCl})$, from which new values of $\lambda^\circ(\text{Cl}^-)$ were derived using Marshall's extrapolated values of Smith and Dismukes' [15] transference numbers for NaCl. Our recent values of λ° for Na^+ , Sr^{2+} , triflate (CF_3SO_3^-) and their ion pairs are based on this correlation [29].

The thermodynamic and transport properties of ions in D_2O have been used to probe hydration effects near ambient conditions [30–35], and they are needed to model corrosion product transport and radiolysis effects in the primary coolant circuits of CANDU heavy-water nuclear reactors [36]. Despite their importance to basic research and the nuclear industry, only one study of experimental limiting conductivities in D_2O has been reported in the literature at temperatures above 373 K [37].

This paper reports experimental values for the conductivities of cations and anions of simple salts in both D_2O and H_2O at temperatures up to 600 K and a pressure of 20 MPa. The purpose of the study was to determine the limiting single-ion conductivities of univalent cations and anions in light and heavy water, up to near-critical conditions, with sufficient precision that differences due to deuterium isotope effects could be compared. The measurements were carried out in the high-precision flow AC conductance cell

constructed at the University of Delaware [18, 20] and modified at the University of Guelph [28, 29, 38]. This instrument has the ability to work at the very low concentrations ($\leq 10^{-3}$ mol·kg $^{-1}$) required to determine accurate limiting conductivities. In addition, the flow feature permits the use of experimental designs that eliminate most systematic errors so that *differences* in the ionic conductivities between different salts in each solvent, and between the same salts in light and heavy water, can be measured with a high degree of precision.

2 Experimental

2.1 Chemicals and Solution Preparation

Stock solutions of ~ 0.1 mol·kg $^{-1}$ NaCl (Alfa Aesar Puratonic, 99.999 %), KCl, (Alfa Aesar 99.95 %), CsCl (Alfa Aesar 99.999 %), KI (Alfa Aesar 99.9 %) and CsI (Alfa Aesar 99.999 %) in light and heavy water were prepared by mass from their anhydrous salts. Each salt was dried at 300 °C until the mass difference between weightings was less than 0.02 %. The stock solutions were prepared by mass with Nanopure light water (resistivity 18.2 M Ω cm) and heavy water provided by Ontario Power Generation Ltd. The D $_2$ O used in solution preparation was determined to be 99.7 mol% D by using a ^1H NMR method, whereby standard additions of glacial HAc (Sigma Aldrich, “99.85 %”) were added to D $_2$ O as an internal reference [39]. Stock solutions in both H $_2$ O and D $_2$ O were prepared in a glove-bag flushed with argon, which was continually kept under positive argon pressure, then stored under an atmosphere of argon until use. The solutions measured in the conductance instrument ($\sim 10^{-3}$ mol·kg $^{-1}$) were prepared by mass dilution under argon from these stock solutions. All solutions were stored and handled under an argon atmosphere to prevent bicarbonate contamination from atmospheric CO $_2$. The bottles were swirled manually to mix the solution and allowed to sit at least for 24 h before the runs. These sample solutions were stored in 250 mL Pyrex glass bottles with KIMAX GL-45 gas-tight tops for no more than 15 days before being injected into the conductance instrument. Each of the gas-tight lids consisted of a septum, an inlet gas tube and a connection port to the conductivity cell.

2.2 AC Conductivity Measurements

Conductivity experiments were carried out using the high-precision AC conductivity flow cell designed by R.H. Wood at the University of Delaware, and described elsewhere [28, 29]. Briefly, the cell consists of a long temperature-controlled platinum inlet tube that leads into a platinized cup that forms the outer electrode. The inner electrode is a platinum rod (electrodeposited with platinum black) that is a direct extension of the platinum tube which carries the exiting solution away from the cell. The entire electrode assembly is contained in a titanium cell body. A sapphire disk and a ceramic spacer provide electrical insulation between the two electrodes. The pressure seal inside the conductivity flow cell is maintained by compressing annealed thin gold disks, which sit between the sapphire insulator and a titanium end-cap, using a system of bolts and Inconel Belleville washers. The temperature of the cell is controlled using three independent systems, capable of regulating to ± 0.15 K over several hours. The first system is an air bath that controls the temperature surrounding the conductivity cell to (5 ± 0.1) K below the temperature of the cell itself. The second system uses heating elements located in the cell body to control the cell

temperature to ± 0.01 K. The third system consists of a co-axial heater placed alongside the incoming platinum tube, and a thermocouple whose junctions are located 1 cm before the exit of the tube and in the cell body, to ensure that the *difference* between the temperature of the incoming fluid and the cell body is less than ± 0.08 K. The temperature of the cell body was measured to an accuracy of ± 0.02 K with a platinum resistance thermometer consisting of a Hart Scientific Model 5612 Probe and a Hart Scientific Model 5707 6½ digit digital multimeter.

Solutions to be analyzed were injected into the flow conductivity cell using the high-pressure liquid chromatography (HPLC) injection system [28, 29] shown in Fig. 1. The first HPLC pump was used to supply a continuous flow of de-gassed and de-ionized water to the instrument at a pressure set by a back-pressure regulator. Two 6-port valves, controlled through a computer, determined whether water from the reservoir flowed directly through the cell, or whether it pushed solution from an injection loop through the cell. The sample to be injected was loaded into the injection loop with a peristaltic pump. The second HPLC pump was then used to pressurize the sample loop by pumping deionized water from the reservoir into the loop, so that the downstream water displaced by the sample in the loop by-passed the cell and flowed directly to the back-pressure regulator. Pressure was measured with a digital pressure transducer (Paroscientific Inc. Model 760-6K) to an accuracy of ± 0.01 MPa. Once the sample was pressurized, the computer switched the 6-port valves to push the sample into the conductivity cell. Experiments were conducted at a flow rate of $0.5 \text{ cm}^3 \cdot \text{min}^{-1}$.

Our study of deuterium isotope effects employed an experimental strategy in which solutions of sodium chloride, potassium chloride, potassium iodide, cesium iodide and cesium chloride, in both H_2O and D_2O , were injected in the sequence shown in Fig. 2, at each temperature, so that systematic errors in the experimental molar conductivities of solutions in the two solvents would cancel, thus yielding more precise values of the

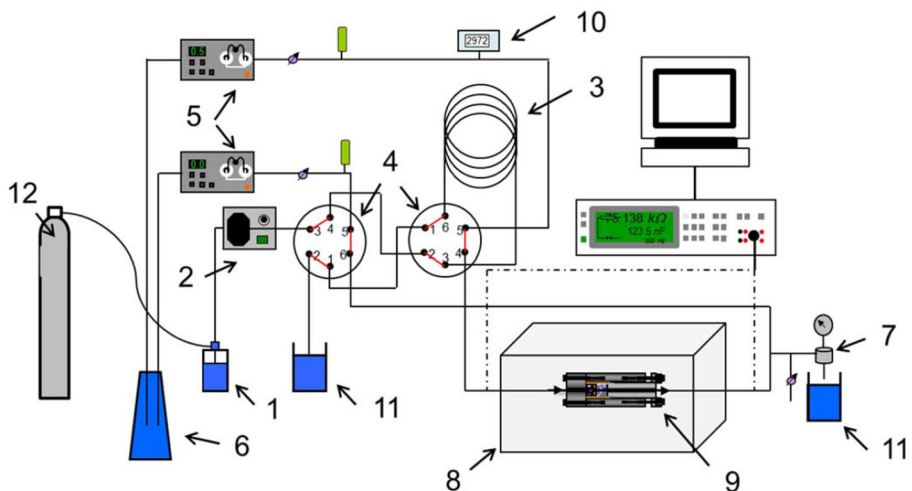


Fig. 1 Schematic of the high pressure sample injection system: (1) Pyrex or Nalgene solution bottles; (2) peristaltic pump; (3) delay loop; (4) six-port injection valves; (5) HPLC pumps; (6) deionized water reservoir; (7) back pressure regulator; (8) temperature-controlled insulated air oven; (9) high temperature conductance cell; (10) pressure transducer; (11) waste solution reservoirs; (12) Argon tank (adapted from Zimmerman et al. [28])

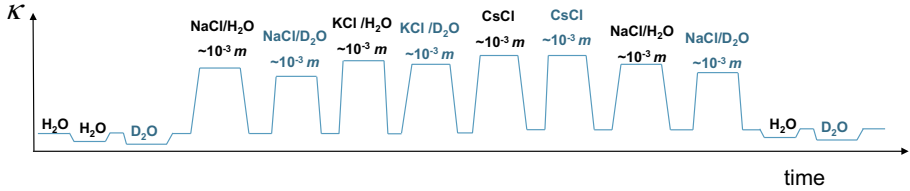


Fig. 2 Experimental design: injection order for set of solutions in the high temperature conductance flow cell

deuterium isotope effect on transport properties. Each series of measurements was started and finished by measuring the conductivity of pure solvents (H_2O and D_2O), and solutions of NaCl in H_2O and D_2O . Measurements were made at temperatures $T = (298, 373, 423, 473, 522, 548, 573 \text{ and } 598) \text{ K}$, at a constant applied pressure of $p \sim 20 \text{ MPa}$. For each aqueous electrolyte solution, after AC impedance data were collected, a long injection of de-ionized and degassed water from the main reservoir, typically $\sim 75\text{--}100 \text{ mL}$, was made to rinse the equipment until the cell conductance had returned to its baseline value. The injection cycle was then repeated with another electrolyte solution.

The complex impedance $Z(\omega)$ of solutions in the conductance cell was measured at frequencies of (100, 200, 500, 1,000, 2,000, 4,000, 6,000, 8,000, and 10,000) Hz using a programmable automatic RCL meter (Fluke Model PM6304C). During the course of each sample injection, at least 80 measurements were taken with a computer over a time span of at least 85 to 100 min. The result of these measurements was a series of values for the real and imaginary impedance, $Z_{\text{Re}}(\omega)$ and $Z_{\text{Im}}(\omega)$ as a function of angular frequency, ω :

$$Z(\omega) = Z_{\text{Re}}(\omega) - j \cdot Z_{\text{Im}}(\omega) \quad (1)$$

where Z is the complex impedance, Z_{Re} and Z_{Im} are the real and imaginary components of the impedance, $j^2 = -1$, and $\omega = 2\pi f$, where f is the frequency. The solution resistance at infinite frequency R_s was found by extrapolation of the linear portion of the Warburg line to the x-axis, as described by Hnedkovsky et al. [20] and Zimmerman and Arcis [40]. The molar conductivities $\Lambda(\text{NaCl})$, measured before and after the series of other salts at each temperature, agreed with one another to within $\pm 1 \%$.

3 Experimental Results

3.1 Conductivity

The experimental conductivity (specific conductance) of the solution, $\kappa_{\text{soln}}^{\text{expt}}$, was calculated from R_s , the resistance of the solution at infinite frequency using the expression:

$$\kappa_{\text{soln}}^{\text{expt}} = \frac{k_{\text{cell}}}{k_s} \quad (2)$$

The cell constant k_{cell} was determined by measuring the conductivity for a series of five KCl(aq) standard solutions (10^{-4} to $10^{-2} \text{ mol}\cdot\text{kg}^{-1}$) at 298.15 K and 20 MPa, then comparing them with reference values from the expression for $\Lambda(\text{KCl}, \text{aq})$ reported by Barthel and his co-workers [41]. Following the procedure used by previous workers

[18–21, 23, 24, 26, 27], the dependence of the cell constant on temperature was calculated from the cell geometry and the thermal expansion coefficient of platinum. The experimental conductivities of the electrolyte solutions, $\kappa_{\text{soln}}^{\text{expt}}$, were corrected for impurities within the solvent and the self-ionization of water by subtracting the experimental values for H_2O , $\kappa_{\text{soln}}^{\text{expt}}$, for each run, using the method of Sharygin et al. [24]:

$$\kappa = \kappa_{\text{soln}}^{\text{expt}} - \kappa_{\text{w}}^{\text{expt}}. \quad (3)$$

3.2 Molar Conductivity and Solution Density

Molar conductivities, Λ^{expt} , were calculated from the corrected specific conductances, κ , using the relationship:

$$\Lambda = \kappa/c \quad (4)$$

where Λ^{expt} is in SI units of $\text{S}\cdot\text{m}^{-2}\cdot\text{mol}^{-1}$. In this study, these were converted to units of $\text{S}\cdot\text{cm}^{-2}\cdot\text{mol}^{-1}$.

The molarity (c) was calculated from the molality (m), molar mass (M) and solution density (ρ_s) using Eq. 5:

$$c = \frac{1000m\rho_s}{mM + 1000} \quad (5)$$

Solution densities were determined from the method developed by Zimmerman et al. [28, 29] which makes use of the Helgeson–Kirkham–Flowers–Tanger (“HKF”) model to estimate the standard partial molar volumes V° of the aqueous species in solution [42–44]. Standard partial molar volumes were calculated using the program SUPCRT [45]. We assumed that partial molar volumes D_2O are the same as those in H_2O . Values for the density, ρ_w , and dielectric constant (relative permittivity), ϵ_w , of water (H_2O) were calculated from the equations of state reported by Wagner and Pruss [46] and Fernandez et al. [47], respectively. The density of heavy water was taken from Hill’s equation of state [48], using the REFPROP software distributed by NIST [49]. The dielectric constant of heavy water was calculated from light water values, using the method reported by Trevani et al. [50].

The experimental conductivities, κ , for the solutions of NaCl, KCl, CsCl, CsI and KI in H_2O and D_2O , and the molar conductivities, Λ^{expt} , calculated from them, are tabulated in Tables 1 and 2, respectively. Values of the cell constant, k_{cell} , for each experimental temperature and also the solvent densities are reported in the tables. The molar conductivities $\Lambda^{\text{expt}}(\text{NaCl})$, measured before and after the series of other salts at each temperature, agreed with one another to within $\pm 1\%$ which we consider to be the precision of our measurements. These values for $\Lambda^{\text{expt}}(\text{NaCl})$ in light and heavy water from $T = 373\text{--}598\text{ K}$ are reported in Table 3. Our experimental values for $\Lambda^\circ(\text{NaCl})$ in H_2O agree with the fitted expression for critically evaluated literature data reported by Zimmerman et al. [28] to better than $\pm 1\%$ from 373 to 523 K, increasing to $\pm 6\%$ at 598 K, within the combined experimental uncertainties. The larger discrepancies above 523 K may reflect the effect of ion pairing or the experimental challenges of working at very high temperatures. The results also agree with the corrected values of $\Lambda^\circ(\text{NaCl})$ in D_2O and H_2O reported by Erickson et al. [37], using this same instrument, to within $\pm 5\%$, except for the values in D_2O at 473, 523 and 548 K which are smaller than our results by 7–10%. The difference lies just outside the combined experimental uncertainties, which are larger

Table 1 Experimental molar conductivities, Λ^{expt} , and limiting molar conductivities, Λ° , for NaCl(aq), KCl(aq), CsCl(aq), KI(aq), and CsI(aq) in H₂O from $T = 298$ to 598 K at $p = 20$ MPa

| Solute | 10^6 m (mol·kg ⁻¹) | 10^6 c (mol·L ⁻¹) | R (Ω) | $10^6 \kappa$ (S·cm ⁻¹) | $\Lambda^{\text{expt,a}}$ (S·cm ² ·mol ⁻¹) | Λ° (S·cm ² ·mol ⁻¹) |
|--|---------------------------------------|--------------------------------------|------------------|--|--|---|
| $T = 298.16$ K, $p = 20.48$ MPa, $\rho_w = 1.00600$ g·cm ⁻³ , $\eta_w = 0.00886$ poise, $\epsilon_r = 79.16$, $k_{\text{cell}} = 0.06590$ cm ⁻¹ , $\kappa_w = 0.984 \times 10^{-6}$ S·cm ⁻¹ | | | | | | |
| NaCl(aq) | 1,027.11 | 1,033.25 | 527.50 | 123.94 | 119.95 ± 1.20 | 122.73 ± 1.23 |
| KCl(aq) | 1,031.87 | 1,038.03 | 438.36 | 149.34 | 143.87 ± 1.44 | 146.84 ± 1.47 |
| KI(aq) | 738.98 | 743.38 | 611.43 | 106.79 | 143.65 ± 1.44 | 146.17 ± 1.46 |
| CsI(aq) | 631.18 | 634.94 | 696.76 | 93.59 | 147.40 ± 1.47 | 149.76 ± 1.50 |
| $T = 373.15$ K, $p = 20.89$ MPa, $\rho_w = 0.96780$ g·cm ⁻³ , $\eta_w = 0.00287$ poise, $\epsilon_r = 56.24$, $k_{\text{cell}} = 0.06360$ cm ⁻¹ , $\kappa_w = 2.061 \times 10^{-6}$ S·cm ⁻¹ | | | | | | |
| NaCl(aq) | 957.86 | 927.00 | 205.85 | 317.80 | 342.83 ± 3.43 | 351.52 ± 3.52 |
| KCl(aq) | 1,080.74 | 1,045.91 | 162.46 | 403.24 | 385.54 ± 3.86 | 395.16 ± 3.95 |
| CsCl(aq) | 1,075.94 | 1,041.25 | 160.17 | 409.03 | 392.82 ± 3.93 | 402.49 ± 4.02 |
| $T = 423.31$ K, $p = 20.20$ MPa, $\rho_w = 0.92765$ g·cm ⁻³ , $\eta_w = 0.00187$ poise, $\epsilon_r = 44.72$, $k_{\text{cell}} = 0.06581$ cm ⁻¹ , $\kappa_w = 3.254 \times 10^{-6}$ S·cm ⁻¹ | | | | | | |
| NaCl(aq) | 1,027.11 | 952.79 | 136.79 | 477.86 | 501.54 ± 5.02 | 515.99 ± 5.16 |
| KCl(aq) | 1,031.87 | 957.19 | 122.82 | 532.60 | 556.42 ± 5.56 | 571.48 ± 5.71 |
| KI(aq) | 738.98 | 685.49 | 173.27 | 376.56 | 549.33 ± 5.49 | 562.08 ± 5.62 |
| CsI(aq) | 631.18 | 585.49 | 201.64 | 323.13 | 551.89 ± 5.52 | 563.72 ± 5.64 |
| $T = 471.98$ K, $p = 20.93$ MPa, $\rho_w = 0.87979$ g·cm ⁻³ , $\eta_w = 0.00140$ poise, $\epsilon_r = 35.73$, $k_{\text{cell}} = 0.06685$ cm ⁻¹ , $\kappa_w = 3.654 \times 10^{-6}$ S·cm ⁻¹ | | | | | | |
| KI(aq) | 1,000.63 | 871.01 | 104.17 | 638.07 | 732.57 ± 7.33 | 758.92 ± 7.59 |
| CsI(aq) | 961.90 | 837.62 | 106.28 | 625.33 | 746.55 ± 7.47 | 772.42 ± 7.72 |
| $T = 473.07$ K, $p = 20.17$ MPa, $\rho_w = 0.87816$ g·cm ⁻³ , $\eta_w = 0.00139$ poise, $\epsilon_r = 35.54$, $k_{\text{cell}} = 0.06578$ cm ⁻¹ , $\kappa_w = 3.978 \times 10^{-6}$ S·cm ⁻¹ | | | | | | |
| NaCl(aq) | 998.01 | 876.41 | 114.09 | 572.56 | 653.31 ± 6.53 | 679.90 ± 6.80 |
| KCl(aq) | 955.23 | 838.83 | 109.09 | 598.99 | 714.07 ± 7.14 | 740.11 ± 7.40 |
| KI(aq) | 1,000.63 | | | | | (763.84 ± 7.64) ^b |
| CsI(aq) | 961.90 | | | | | (777.43 ± 7.77) ^b |
| $T = 523.56$ K, $p = 21.14$ MPa, $\rho_w = 0.81565$ g·cm ⁻³ , $\eta_w = 0.00110$ poise, $\epsilon_r = 28.13$, $k_{\text{cell}} = 0.06681$ cm ⁻¹ , $\kappa_w = 3.961 \times 10^{-6}$ S·cm ⁻¹ | | | | | | |
| KI(aq) | 528.48 | 428.65 | 176.01 | 375.64 | 876.33 ± 8.76 | 895.49 ± 8.95 |
| CsI(aq) | 631.69 | 511.78 | 145.43 | 455.45 | 889.94 ± 8.90 | 910.84 ± 9.11 |
| $T = 522.88$ K, $p = 20.19$ MPa, $\rho_w = 0.81666$ g·cm ⁻³ , $\eta_w = 0.00111$ poise, $\epsilon_r = 35.54$, $k_{\text{cell}} = 0.06574$ cm ⁻¹ , $\kappa_w = 4.085 \times 10^{-6}$ S·cm ⁻¹ | | | | | | |
| NaCl(aq) | 1,101.58 | 899.62 | 92.26 | 708.49 | 787.54 ± 7.88 | 821.78 ± 8.22 |
| KCl(aq) | 955.23 | 780.10 | 98.43 | 663.86 | 850.99 ± 8.51 | 883.03 ± 8.83 |
| CsCl(aq) | 1,073.79 | 876.91 | 86.37 | 757.09 | 863.37 ± 8.63 | 897.21 ± 8.97 |
| KI(aq) | 528.48 | | | | | (894.39 ± 8.94) ^c |
| CsI(aq) | 631.69 | | | | | (907.54 ± 9.08) ^c |
| $T = 548.59$ K, $p = 20.15$ MPa, $\rho_w = 0.77819$ g·cm ⁻³ , $\eta_w = 0.00100$ poise, $\epsilon_r = 24.40$, $k_{\text{cell}} = 0.06679$ cm ⁻¹ , $\kappa_w = 3.704 \times 10^{-6}$ S·cm ⁻¹ | | | | | | |
| KI(aq) | 736.44 | 568.61 | 122.86 | 539.95 | 949.60 ± 9.50 | 971.96 ± 9.72 |
| CsI(aq) | 631.69 | 488.27 | 142.76 | 464.19 | 950.68 ± 9.51 | 971.44 ± 9.71 |

Table 1 continued

| Solute | 10^6 m (mol·kg ⁻¹) | 10^6 c (mol·L ⁻¹) | R (Ω) | 10^6 κ (S·cm ⁻¹) | $A^{\text{expt.a}}$ (S·cm ² ·mol ⁻¹) | A° (S·cm ² ·mol ⁻¹) |
|--|---------------------------------------|--------------------------------------|---------|--|--|---|
| $T = 548.10$ K, $p = 20.93$ MPa, $\rho_w = 0.78000$ g·cm ⁻³ , $\eta_w = 0.00100$ poise, $\epsilon_r = 24.49$, $k_{\text{cell}} = 0.06349$ cm ⁻¹ , $\kappa_w = 3.551 \times 10^{-6}$ S·cm ⁻¹ | | | | | | |
| NaCl(aq) | 1,124.57 | 877.19 | 87.63 | 720.95 | 821.89 ± 8.22 | 860.20 ± 8.60 |
| KCl(aq) | 1,080.74 | 842.99 | 84.88 | 744.47 | 883.13 ± 8.83 | 920.75 ± 9.21 |
| CsCl(aq) | 1,075.94 | 839.24 | 83.17 | 759.78 | 905.32 ± 9.05 | 942.87 ± 9.43 |
| KI(aq) | 736.44 | | | | | (967.88 ± 9.68) ^d |
| CsI(aq) | 631.69 | | | | | (967.36 ± 9.67) ^d |
| $T = 572.80$ K, $p = 20.77$ MPa, $\rho_w = 0.73670$ g·cm ⁻³ , $\eta_w = 0.00090$ poise, $\epsilon_r = 21.22$, $k_{\text{cell}} = 0.06347$ cm ⁻¹ , $\kappa_w = 2.944 \times 10^{-6}$ S·cm ⁻¹ | | | | | | |
| NaCl(aq) | 964.37 | 710.49 | 100.42 | 629.15 | 885.53 ± 8.86 | 925.42 ± 9.25 |
| KCl(aq) | 1,091.88 | 804.43 | 83.47 | 757.45 | 941.61 ± 9.42 | 983.81 ± 9.84 |
| CsCl(aq) | 1,137.31 | 837.88 | 78.94 | 801.14 | 956.15 ± 9.56 | 999.14 ± 9.99 |
| $T = 597.93$ K, $p = 20.74$ MPa, $\rho_w = 0.68230$ g·cm ⁻³ , $\eta_w = 0.00081$ poise, $\epsilon_r = 17.87$, $k_{\text{cell}} = 0.06346$ cm ⁻¹ , $\kappa_w = 2.070 \times 10^{-6}$ S·cm ⁻¹ | | | | | | |
| NaCl(aq) | 787.31 | 537.22 | 123.69 | 510.96 | 951.11 ± 9.51 | 992.64 ± 9.93 |
| KCl(aq) | 1,091.88 | 745.06 | 85.02 | 744.32 | 999.00 ± 9.99 | 1,047.07 ± 10.47 |
| CsCl(aq) | 1,137.31 | 776.05 | 80.30 | 788.15 | 1,015.59 ± 10.16 | 1,064.52 ± 10.65 |

Values for KI_(aq) and CsI_(aq) in parenthesis were adjusted to the experimental temperature of the other salts using the Walden product ratio (Eq. 19)

^a The reported errors for the limiting conductivity correspond to our experimental precision. The absolute accuracy from 298 to 523 K is estimated to be ±3 %, rising to ±6 % at 598 K

^b Corrected from the results at 471.98 K and 20.83 MPa using the Walden product ratio (Eq. 19)

^c Corrected from the results at 523.56 K and 21.14 MPa using the Walden product ratio (Eq. 19)

^d Corrected from the results at 548.59 K and 20.74 MPa using the Walden product ratio (Eq. 19)

for Erickson’s study. From these comparisons, we consider the absolute accuracy of the conductivity measurements from 298 to 523 K to be ±3 %, rising to ±6 % at 598 K.

3.3 Limiting Molar Conductivity

The limiting molar conductivities, A° were calculated from A^{expt} using the Fuoss–Hsia–Fernández-Prini (“FHFP”) conductivity model [51], which is the classical polynomial expansion of the Fuoss–Hsia equation for the special case of symmetrical electrolytes:

$$A = A^\circ - S \cdot c^{1/2} + E \cdot c \cdot \ln(c) + J_1 \cdot c - J_2 \cdot c^{3/2} \tag{6}$$

Here, S is the Onsager limiting slope, and the expressions for E , J_1 and J_2 are given by Fernández-Prini [51]. The terms S , E , J_1 , and J_2 all depend on A° . The E and J terms also depend on the distance of closest approach, a , which we defined by the Bjerrum distance, q_B :

$$q_B = 2a = \frac{(z \cdot e)^2}{\epsilon_w \cdot k_B \cdot T} \tag{7}$$

This treatment for the concentration dependence of A has been evaluated by Bianchi et al. [52], and has been shown to yield values that are accurate to ~1 % over the range 0–0.1 mol·cm⁻³. Details can be found elsewhere [28, 29]. Our extrapolation to infinite

Table 2 Experimental molar conductivities, Λ^{expt} , and limiting molar conductivities, Λ° , for NaCl(aq), KCl(aq), CsCl(aq), KI(aq), and CsI(aq) in D₂O from $T = 298$ to 598 K at $p = 20$ MPa

| Solute | 10^6 m (mol·kg ⁻¹) | 10^6 c (mol·L ⁻¹) | R (Ω) | 10^6 κ (S·cm ⁻¹) | $\Lambda^{\text{expt. a}}$ (S·cm ² ·mol ⁻¹) | Λ° (S·cm ² ·mol ⁻¹) |
|--|---------------------------------------|--------------------------------------|------------------|--|---|--|
| $T = 298.16$ K, $p = 20.48$ MPa, $\rho_{\text{D}_2\text{O}} = 1.11479$ g·cm ⁻³ , $\eta_{\text{D}_2\text{O}} = 0.01088$ poise, $\epsilon_r = 78.96$, $k_{\text{cell}} = 0.06590$ cm ⁻¹ , $\kappa_w = 0.578 \times 10^{-6}$ S·cm ⁻¹ | | | | | | |
| NaCl(aq) | 919.32 | 1,024.84 | 638.99 | 102.55 | 100.06 ± 1.00 | 102.34 ± 1.02 |
| KCl(aq) | 1,234.75 | 1,376.43 | 383.15 | 171.41 | 124.53 ± 1.25 | 127.37 ± 1.27 |
| KI(aq) | 671.52 | 748.58 | 725.85 | 90.21 | 120.50 ± 1.21 | 122.59 ± 1.23 |
| CsI(aq) | 628.90 | 701.06 | 765.04 | 85.56 | 122.04 ± 1.22 | 124.07 ± 1.24 |
| $T = 373.15$ K, $p = 20.89$ MPa, $\rho_{\text{D}_2\text{O}} = 1.07390$ g·cm ⁻³ , $\eta_{\text{D}_2\text{O}} = 0.00336$ poise, $\epsilon_r = 56.00$, $k_{\text{cell}} = 0.06360$ cm ⁻¹ , $\kappa_w = 1.886 \times 10^{-6}$ S·cm ⁻¹ | | | | | | |
| NaCl(aq) | 870.66 | 934.99 | 232.15 | 281.75 | 301.34 ± 3.01 | 308.90 ± 3.09 |
| KCl(aq) | 1,284.94 | 1,379.84 | 141.32 | 464.04 | 336.30 ± 3.36 | 345.79 ± 3.46 |
| CsCl(aq) | 1,025.92 | 1,101.69 | 174.56 | 375.32 | 340.68 ± 3.41 | 349.24 ± 3.49 |
| $T = 423.31$ K, $p = 20.20$ MPa, $\rho_{\text{D}_2\text{O}} = 1.02919$ g·cm ⁻³ , $\eta_{\text{D}_2\text{O}} = 0.00216$ poise, $\epsilon_r = 44.51$, $k_{\text{cell}} = 0.06581$ cm ⁻¹ , $\kappa_w = 2.209 \times 10^{-6}$ S·cm ⁻¹ | | | | | | |
| NaCl(aq) | 919.32 | 946.15 | 156.04 | 421.96 | 443.43 ± 4.43 | 456.04 ± 4.56 |
| KCl(aq) | 1,234.75 | 1,270.75 | 103.67 | 632.64 | 497.84 ± 4.98 | 513.00 ± 5.13 |
| KI(aq) | 920.23 | 947.05 | 142.20 | 460.61 | 486.37 ± 4.86 | 499.41 ± 4.99 |
| CsI(aq) | 628.90 | 647.23 | 208.28 | 313.76 | 484.78 ± 4.85 | 495.63 ± 4.96 |
| $T = 471.98$ K, $p = 20.93$ MPa, $\rho_{\text{D}_2\text{O}} = 0.97530$ g·cm ⁻³ , $\eta_{\text{D}_2\text{O}} = 0.00159$ poise, $\epsilon_r = 35.58$, $k_{\text{cell}} = 0.06684$ cm ⁻¹ , $\kappa_w = 13.0681 \times 10^{-6}$ S·cm ⁻¹ | | | | | | |
| KI(aq) | 958.20 | 923.83 | 116.68 | 559.84 | 606.00 ± 6.06 | 631.70 ± 6.32 |
| CsI(aq) | 662.38 | 641.07 | 164.85 | 392.44 | 612.16 ± 6.12 | 633.80 ± 6.34 |
| $T = 473.07$ K, $p = 20.17$ MPa, $\rho_{\text{D}_2\text{O}} = 0.97344$ g·cm ⁻³ , $\eta_{\text{D}_2\text{O}} = 0.00158$ poise, $\epsilon_r = 35.38$, $k_{\text{cell}} = 0.06578$ cm ⁻¹ , $\kappa_w = 2.898 \times 10^{-6}$ S·cm ⁻¹ | | | | | | |
| NaCl(aq) | 978.43 | 952.44 | 117.12 | 501.96 | 586.63 ± 5.87 | 612.86 ± 6.13 |
| KCl(aq) | 1,313.77 | 1,278.85 | 81.66 | 802.61 | 627.60 ± 6.28 | 657.63 ± 6.58 |
| KI(aq) | 958.20 | | | | | (636.07 ± 6.36) ^b |
| CsI(aq) | 662.38 | | | | | (638.18 ± 6.38) ^b |
| $T = 523.56$ K, $p = 21.14$ MPa, $\rho_{\text{D}_2\text{O}} = 0.90272$ g·cm ⁻³ , $\eta_{\text{D}_2\text{O}} = 0.00123$ poise, $\epsilon_r = 27.94$, $k_{\text{cell}} = 0.06681$ cm ⁻¹ , $\kappa_w = 3.158 \times 10^{-6}$ S·cm ⁻¹ | | | | | | |
| KI(aq) | 354.46 | 318.63 | 262.55 | 251.32 | 788.75 ± 7.89 | 804.46 ± 8.04 |
| CsI(aq) | 656.44 | 588.09 | 139.07 | 477.25 | 811.53 ± 8.12 | 832.68 ± 8.33 |
| $T = 522.88$ K, $p = 20.19$ MPa, $\rho_{\text{D}_2\text{O}} = 0.90392$ g·cm ⁻³ , $\eta_{\text{D}_2\text{O}} = 0.00123$ poise, $\epsilon_r = 27.80$, $k_{\text{cell}} = 0.06574$ cm ⁻¹ , $\kappa_w = 3.271 \times 10^{-6}$ S·cm ⁻¹ | | | | | | |
| NaCl(aq) | 9,842.90 | 889.73 | 103.70 | 630.69 | 708.86 ± 7.09 | 741.38 ± 7.41 |
| KCl(aq) | 1,313.77 | 1,187.55 | 73.28 | 893.89 | 752.72 ± 7.53 | 789.63 ± 7.90 |
| CsCl(aq) | 954.43 | 862.72 | 98.65 | 663.14 | 768.66 ± 7.69 | 800.72 ± 8.01 |
| KI(aq) | 354.46 | | | | | (801.71 ± 8.02) ^c |
| CsI(aq) | 656.44 | | | | | (829.84 ± 8.30) ^c |
| $T = 548.59$ K, $p = 20.15$ MPa, $\rho_{\text{D}_2\text{O}} = 0.86035$ g·cm ⁻³ , $\eta_{\text{D}_2\text{O}} = 0.00110$ poise, $\epsilon_r = 24.30$, $k_{\text{cell}} = 0.06679$ cm ⁻¹ , $\kappa_w = 3.044 \times 10^{-6}$ S·cm ⁻¹ | | | | | | |
| KI(aq) | 633.05 | 540.52 | 140.77 | 471.44 | 872.19 ± 8.72 | 892.87 ± 8.93 |
| CsI(aq) | 656.44 | 560.48 | 135.63 | 489.44 | 873.24 ± 8.73 | 894.28 ± 8.94 |

Table 2 continued

| Solute | 10^6 m (mol·kg ⁻¹) | 10^6 c (mol·L ⁻¹) | R (Ω) | 10^6 κ (S·cm ⁻¹) | $\Lambda^{\text{expt, a}}$ (S·cm ² ·mol ⁻¹) | Λ° (S·cm ² ·mol ⁻¹) |
|--|---------------------------------------|--------------------------------------|---------|--|---|--|
| $T = 548.10$ K, $p = 20.93$ MPa, $\rho_{\text{D}_2\text{O}} = 0.86231$ g·cm ⁻³ , $\eta_{\text{D}_2\text{O}} = 0.00110$ poise, $\epsilon_r = 24.38$, $k_{\text{cell}} = 0.06349$ cm ⁻¹ , $\kappa_w = 3.044 \times 10^{-6}$ S·cm ⁻¹ | | | | | | |
| NaCl(aq) | 997.10 | 859.84 | 98.58 | 641.01 | 745.50 ± 7.46 | 781.89 ± 7.82 |
| KCl(aq) | 1,284.94 | 1,108.04 | 72.39 | 874.05 | 788.82 ± 7.89 | 829.42 ± 8.29 |
| CsCl(aq) | 1,025.92 | 884.67 | 88.79 | 712.01 | 804.83 ± 8.05 | 841.65 ± 8.42 |
| KI(aq) | 633.05 | | | | | (888.99 ± 8.89) ^d |
| CsI(aq) | 656.44 | | | | | (890.39 ± 8.90) ^d |
| $T = 572.80$ K, $p = 20.77$ MPa, $\rho_{\text{D}_2\text{O}} = 0.81312$ g·cm ⁻³ , $\eta_{\text{D}_2\text{O}} = 0.00099$ poise, $\epsilon_r = 21.10$, $k_{\text{cell}} = 0.06347$ cm ⁻¹ , $\kappa_w = 2.604 \times 10^{-6}$ S·cm ⁻¹ | | | | | | |
| NaCl(aq) | 943.20 | 766.98 | 102.27 | 618.02 | 805.79 ± 8.06 | 845.47 ± 8.45 |
| KCl(aq) | 1,276.10 | 1,037.68 | 72.51 | 872.80 | 841.11 ± 8.41 | 886.31 ± 8.86 |
| CsCl(aq) | 1,040.78 | 846.30 | 86.82 | 728.45 | 860.75 ± 8.61 | 902.29 ± 9.02 |
| $T = 597.93$ K, $p = 20.74$ MPa, $\rho_{\text{D}_2\text{O}} = 0.75062$ g·cm ⁻³ , $\eta_{\text{D}_2\text{O}} = 0.00088$ poise, $\epsilon_r = 17.71$, $k_{\text{cell}} = 0.06346$ cm ⁻¹ , $\kappa_w = 1.953 \times 10^{-6}$ S·cm ⁻¹ | | | | | | |
| NaCl(aq) | 754.05 | 566.05 | 127.63 | 495.24 | 874.90 ± 8.75 | 916.09 ± 9.16 |
| KCl(aq) | 1,276.10 | 957.98 | 73.96 | 856.06 | 893.61 ± 8.94 | 945.10 ± 9.45 |
| CsCl(aq) | 1,040.78 | 781.29 | 88.12 | 718.13 | 919.15 ± 9.19 | 966.73 ± 9.67 |

Values for KI_(aq) and CsI_(aq) in parenthesis were adjusted to the experimental temperature of the other salts using the Walden product ratio (Eq. 19)

^a The reported errors for the limiting conductivity correspond to our experimental precision. The absolute accuracy from 298 to 523 K is estimated to be ±3 %, rising to ±6 % at 598 K

^b Corrected from the results at 471.98 K and 20.83 MPa using the Walden product ratio (Eq. 19)

^c Corrected from the results at 523.56 K and 21.14 MPa using the Walden product ratio (Eq. 19)

^d Corrected from the results at 548.59 K and 20.74 MPa using the Walden product ratio (Eq. 19)

dilution for obtaining limiting molar conductivities was done with a single experimental data point, measured at an ionic strength of $\sim 10^{-3}$ mol·kg⁻¹. This method can only be applied at conditions where ion association is negligible.

The limiting molar conductivities of each salt in both H₂O and D₂O are tabulated in Tables 1 and 2. The solvent properties used to carry out our calculations are reported in Table 4.

4 Single-Ion Limiting Molar Conductivities under Hydrothermal Conditions

4.1 Transference Number Extrapolations in H₂O

The determination of the limiting equivalent conductivities of individual ions from the molar conductivity data in Tables 1 and 2 requires a value for the transference number of the chloride ion at infinite dilution, $t^\circ(\text{Cl}^-)$, according to the relationship:

$$\lambda^\circ(\text{Cl}^-) = t^\circ(\text{Cl}^-) \cdot \Lambda^\circ(\text{M}^+\text{Cl}^-), \tag{8}$$

Table 3 Experimental sodium chloride molar conductivities, $\Lambda(\text{NaCl})$, collected at the beginning and at the end of each experimental run in H_2O and D_2O , from $T = 298$ to 598 K at $p = 20$ MPa

| T (K) | p (MPa) | 10^6 m ($\text{mol}\cdot\text{kg}^{-1}$) | 10^6 c ($\text{mol}\cdot\text{L}^{-1}$) | $\Lambda(\text{NaCl})$ #1 ($\text{S}\cdot\text{cm}^2\cdot\text{mol}^{-1}$) | $\Lambda(\text{NaCl})$ #2 ($\text{S}\cdot\text{cm}^2\cdot\text{mol}^{-1}$) |
|---------|-----------|---|--|---|---|
| 298.16 | 20.48 | 1,027.11 | 1,033.25 | 119.95 | NA |
| 373.15 | 20.89 | 957.86 | 927.00 | 342.83 | 346.32 |
| 423.31 | 20.20 | 1,027.11 | 952.79 | 501.54 | 507.63 |
| 473.07 | 20.17 | 998.01 | 876.41 | 653.31 | 660.91 |
| 522.88 | 20.19 | 1,101.58 | 899.62 | 787.54 | 787.65 |
| 548.10 | 20.93 | 1,124.57 | 877.19 | 821.89 | 821.42 |
| 572.80 | 20.77 | 964.37 | 710.49 | 885.53 | 885.04 |
| 597.93 | 20.74 | 787.31 | 537.22 | 951.11 | 953.91 |
| 298.16 | 20.48 | 919.32 | 1,024.84 | 100.06 | NA |
| 373.15 | 20.89 | 870.66 | 934.99 | 301.34 | 301.40 |
| 423.31 | 20.20 | 919.32 | 946.15 | 443.43 | 445.52 |
| 473.07 | 20.17 | 1,147.37 | 1,116.89 | 586.63 | 590.88 |
| 522.88 | 20.19 | 933.53 | 843.85 | 708.86 | 712.26 |
| 548.10 | 20.93 | 1,124.57 | 877.19 | 745.50 | 744.47 |
| 572.80 | 20.77 | 943.20 | 766.98 | 805.79 | 806.05 |
| 597.93 | 20.74 | 754.05 | 566.05 | 874.90 | 878.43 |

Table 4 Density (ρ), viscosity (η), dielectric constant (ϵ_r) and pK of H_2O and D_2O from $T = 298$ to 598 K at $p = 20$ MPa

| T (K) | p (MPa) | $\rho_{\text{H}_2\text{O}}$ ($\text{g}\cdot\text{cm}^{-3}$) | $\eta_{\text{H}_2\text{O}}$ (poise) | $\epsilon_{r,\text{H}_2\text{O}}$ | $pK_{\text{H}_2\text{O}}$ | $\rho_{\text{D}_2\text{O}}$ ($\text{g}\cdot\text{cm}^{-3}$) | $\eta_{\text{D}_2\text{O}}$ (poise) | $\epsilon_{r,\text{D}_2\text{O}}$ | $pK_{\text{D}_2\text{O}}$ |
|---------|-----------|--|--|-----------------------------------|---------------------------|--|--|-----------------------------------|---------------------------|
| 298.16 | 20.48 | 1.00600 | 0.00886 | 79.16 | 13.920 | 1.11479 | 0.01088 | 78.96 | 13.060 |
| 373.15 | 20.89 | 0.96780 | 0.00287 | 56.24 | 12.190 | 1.07390 | 0.00336 | 56.00 | 11.440 |
| 423.31 | 20.20 | 0.92765 | 0.00187 | 44.72 | 11.560 | 1.02919 | 0.00216 | 44.51 | 10.850 |
| 473.07 | 20.17 | 0.87816 | 0.00139 | 35.54 | 11.190 | 0.97344 | 0.00158 | 35.38 | 10.510 |
| 522.88 | 20.19 | 0.81666 | 0.00111 | 27.91 | 11.060 | 0.90392 | 0.00123 | 27.80 | 10.410 |
| 548.10 | 20.93 | 0.78000 | 0.00100 | 24.49 | 11.080 | 0.86231 | 0.00110 | 24.38 | 10.450 |
| 572.80 | 20.77 | 0.73670 | 0.00090 | 21.22 | 11.200 | 0.81312 | 0.00099 | 21.10 | 10.580 |
| 597.93 | 20.74 | 0.68230 | 0.00081 | 17.87 | 11.450 | 0.75062 | 0.00088 | 17.71 | 11.220 |

where $M^+ = \text{Na}^+$ or K^+ . While many transference number measurements have been made under ambient conditions [53–56], the only transference number measurements reported at elevated temperatures are those of Smith and Dismukes [15, 57], who measured values for $t(\text{Cl}^-)$ in $\text{NaCl}(\text{aq})$ and $\text{KCl}(\text{aq})$ up to 398 and 388 K, respectively. These are the highest temperatures ever reported for accurate transference number measurements of 1:1 salts.

Following the treatment in their original papers, experimental transference numbers for the chloride ion in NaCl and KCl from Smith and Dismukes are plotted in Fig. 3a, b as $\log_{10} \{t^\circ(\text{Cl}^-)/[t^\circ(M^+)]\}$ versus $1/T$, along with values for NaCl from Allgood and Gordon [56] and Longworth [53], and values for KCl from Allgood et al. [55] and

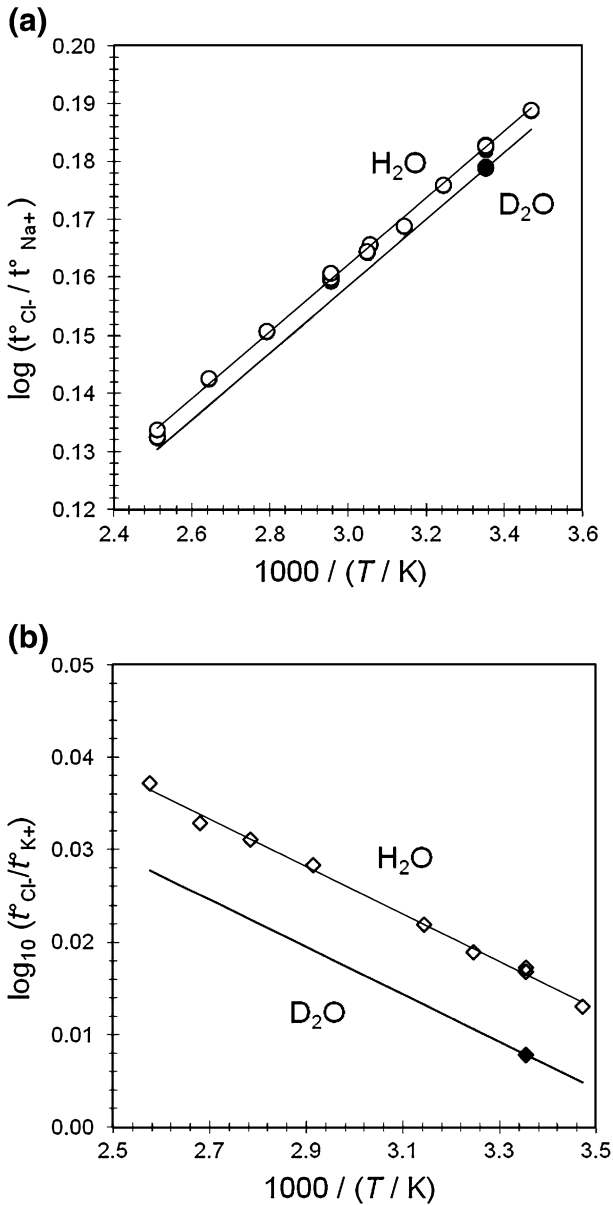


Fig. 3 Temperature dependence of transference numbers in H₂O and D₂O. **a** Values for NaCl: *open circle*, Smith and Dismukes [15]; *filled circle*, Swain and Evans [30]. **b** Values for KCl: *open diamond*, Smith and Dismukes [57]; *filled diamond*, Nakahara et al. [59]

MacInnes and Longworth [54]. Least-squares fits to these data yield the following linear relationships for NaCl and KCl with regression coefficients $R^2 = 0.998$ and 0.995 , respectively:

$$\log_{10} \left(\frac{t_{\text{Cl}^-}^{\circ}}{t_{\text{Na}^+}^{\circ}} \right) = \frac{55.57}{T} - 0.01049 \quad (9)$$

and

$$\log_{10} \left(\frac{t_{\text{Cl}^-}^{\circ}}{t_{\text{K}^+}^{\circ}} \right) = -\frac{25.68}{T} + 0.1027 \quad (10)$$

The classic compilations of single ion conductivities in hydrothermal solutions by Quist and Marshall [10] and Marshall [13, 14], and more recent studies by Zimmerman et al. [28, 29], are based on values of $\lambda^{\circ}(\text{Cl}^-)$ derived by extrapolating Eq. 10 to temperatures as high as 1,073 K.

4.2 Transference Number Extrapolations in D₂O

Measurements for transference numbers in D₂O are much more rare than those in H₂O. Values have been reported for NaCl at 298 K [30] and for KCl at 288 K [58], 298 K [59] and 318 K [60]. Because literature values for $t^{\circ}(\text{Cl}^-)$ in D₂O are only available near ambient conditions, we adopted the assumption that their temperature dependence in aqueous NaCl and KCl solutions is the same as that in light water, as expressed by Eqs. 9 and 10. Combining this assumption with the values at 298.15 K reported by Swain and Evans [30] for NaCl and by Nakahara et al. [59] for KCl, yields the expressions:

$$\log_{10} \left(\frac{t_{\text{Cl}^-}^{\circ}}{t_{\text{Na}^+}^{\circ}} \right) = \frac{55.57}{T} - 0.01416 \quad (11)$$

and

$$\log_{10} \left(\frac{t_{\text{Cl}^-}^{\circ}}{t_{\text{K}^+}^{\circ}} \right) = -\frac{25.68}{T} + 0.09394 \quad (12)$$

The resulting extrapolated values $t^{\circ}(\text{Cl}^-)$ for NaCl and KCl are plotted in Fig. 3a, b, respectively.

The values used for $t_{\text{Cl}^-}^{\circ}$ in H₂O and in D₂O in our subsequent calculations are tabulated in Tables 5 and 6.

4.3 The Limiting Conductivity of the Chloride Ion, $\lambda^{\circ}(\text{Cl}^-)$

The extrapolated expressions for transference numbers, Eqs. 9 and 10, were used to calculate the limiting molar conductivity of the chloride ion, $\lambda^{\circ}(\text{Cl}^-)$, from the experimental molar conductivities $\Lambda^{\circ}(\text{NaCl})$ and $\Lambda^{\circ}(\text{KCl})$ in light water, listed in Table 1. The results are plotted in Fig. 4. The figure also includes a plot of the expression for $\lambda^{\circ}(\text{Cl}^-)$ derived by Zimmerman et al. [28] from their critically evaluated compilation of conductivity literature data for NaCl. These were based on transference numbers reported by Marshall, which were derived from a linear fit to Smith and Dismukes' data, analogous to Eq. 9. Figure 4 also includes values of $\lambda^{\circ}(\text{Cl}^-)$ at higher temperatures, calculated from the limiting conductivities $\Lambda^{\circ}(\text{NaCl})$ and $\Lambda^{\circ}(\text{KCl})$ reported by Ref. [21] from 570 to 673 K. These studies were done at different pressures (NaCl, $p = 32.53$ MPa; KCl,

Table 5 Single ion limiting conductivities, λ° , for Cl^- , K^+ , Na^+ , Cs^+ and I^- in H_2O from $T = 298$ to 598 K at $p = 20$ MPa

| T (K) | $\lambda^\circ(\text{Cl}^-)^a$ ($\text{S}\cdot\text{cm}^2\cdot\text{mol}^{-1}$) | $\lambda^\circ(\text{Cl}^-)^b$ ($\text{S}\cdot\text{cm}^2\cdot\text{mol}^{-1}$) | $\lambda^\circ(\text{Na}^+)$ ($\text{S}\cdot\text{cm}^2\cdot\text{mol}^{-1}$) | $\lambda^\circ(\text{K}^+)$ ($\text{S}\cdot\text{cm}^2\cdot\text{mol}^{-1}$) | $\lambda^\circ(\text{Cs}^+)^c$ ($\text{S}\cdot\text{cm}^2\cdot\text{mol}^{-1}$) | $\lambda^\circ(\text{I}^-)$ ($\text{S}\cdot\text{cm}^2\cdot\text{mol}^{-1}$) | $\lambda^\circ(\text{Cs}^+)^d$ ($\text{S}\cdot\text{cm}^2\cdot\text{mol}^{-1}$) |
|-------------------------------------|--|--|--|---|--|---|--|
| 298.162 | 0.5095 | 74.82 | 47.91 | 72.02 | – | 74.15 | 75.60 |
| 373.150 | 0.5195 | 205.28 | 146.25 | 189.88 | 197.21 | – | – |
| 423.308 | 0.5242 | 299.55 | 216.44 | 271.93 | – | 290.15 | 273.57 |
| 473.074 | 0.5278 | 390.65 | 289.25 | 349.46 | – | 405.89 | 366.54 |
| 522.876 | 0.5308 | 468.70 | 353.08 | 414.33 | 428.50 | 439.26 | 471.57 |
| 548.100 | 0.5321 | 489.92 | 370.28 | 430.83 | 452.95 | 505.60 | 465.84 |
| 572.800 | 0.5332 | 524.61 | 400.81 | 459.20 | 474.53 | – | – |
| 597.931 | 0.5343 | 559.47 | 433.17 | 487.60 | 505.05 | – | – |
| $\delta\lambda^\circ/\lambda^\circ$ | | ± 0.010 | ± 0.014 | ± 0.010 | ± 0.014 | ± 0.014 | ± 0.017 |

^a Calculated from Eq. 10

^b Derived from $\lambda^\circ(\text{KCl})$

^c Derived from $\lambda^\circ(\text{CsCl})$

^d Derived from $\lambda^\circ(\text{CsI})$

^e Precision relative to other ions measured in this work

Table 6 Single ion limiting conductivities, λ° , for Cl^- , K^+ , Na^+ , Cs^+ and Γ^- in D_2O from $T = 298$ to 598 K at $p = 20$ MPa

| T (K) | $\lambda^\circ(\text{Cl}^-)^a$ ($\text{S}\cdot\text{cm}^2\cdot\text{mol}^{-1}$) | $\lambda^\circ(\text{Cl}^-)^b$ ($\text{S}\cdot\text{cm}^2\cdot\text{mol}^{-1}$) | $\lambda^\circ(\text{Na}^+)$ ($\text{S}\cdot\text{cm}^2\cdot\text{mol}^{-1}$) | $\lambda^\circ(\text{K}^+)$ ($\text{S}\cdot\text{cm}^2\cdot\text{mol}^{-1}$) | $\lambda^\circ(\text{Cs}^+)^c$ ($\text{S}\cdot\text{cm}^2\cdot\text{mol}^{-1}$) | $\lambda^\circ(\Gamma^-)$ ($\text{S}\cdot\text{cm}^2\cdot\text{mol}^{-1}$) | $\lambda^\circ(\text{Cs}^+)^d$ ($\text{S}\cdot\text{cm}^2\cdot\text{mol}^{-1}$) |
|-------------------------------------|--|--|--|---|--|---|--|
| 298.162 | 0.5045 | 64.26 | 38.08 | 63.11 | – | 59.48 | 64.59 |
| 373.150 | 0.5145 | 177.89 | 131.01 | 167.89 | 171.35 | – | – |
| 423.308 | 0.5191 | 266.32 | 189.72 | 246.68 | – | 252.74 | 242.89 |
| 473.074 | 0.5228 | 343.82 | 269.04 | 313.81 | – | 319.08 | 314.72 |
| 522.876 | 0.5258 | 415.17 | 326.21 | 374.45 | 385.55 | 416.57 | 416.11 |
| 548.100 | 0.5271 | 437.17 | 344.72 | 392.25 | 404.48 | 470.02 | 424.26 |
| 572.800 | 0.5282 | 468.19 | 377.29 | 418.12 | 434.11 | – | – |
| 597.931 | 0.5293 | 500.26 | 415.83 | 444.84 | 466.47 | – | – |
| $\delta\lambda^\circ/\lambda^\circ$ | | ± 0.010 | ± 0.014 | ± 0.010 | ± 0.014 | ± 0.014 | ± 0.017 |

^a Calculated from Eq. 10^b Derived from $\lambda^\circ(\text{KCl})$ ^c Derived from $\lambda^\circ(\text{CsCl})$ ^d Derived from $\lambda^\circ(\text{CsI})$ ^e Precision relative to other ions measured in this work

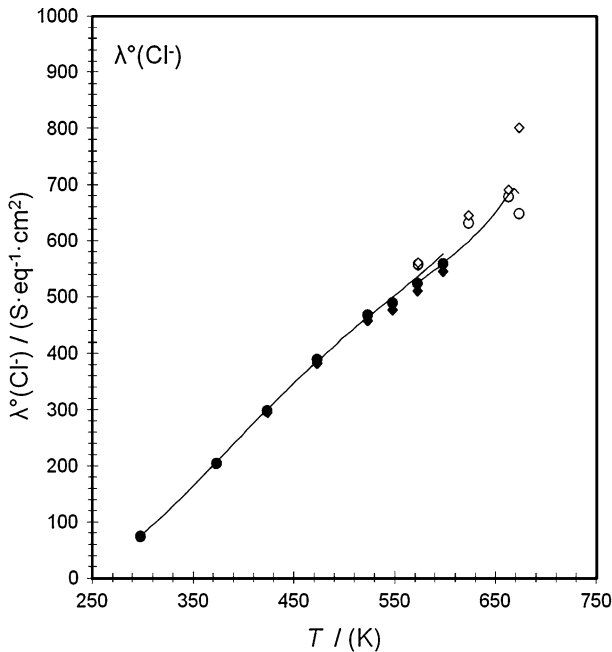


Fig. 4 Experimental limiting single ion conductivity for chloride in H_2O as a function of temperature: *filled circle*, this work $p = 20$ MPa, $\lambda^\circ(\text{Cl}^-)$ derived using KCl transference numbers; *filled diamond*, this work $p = 20$ MPa, $\lambda^\circ(\text{Cl}^-)$ derived using NaCl transference number; *open circle*, Ho et al. [21] $p = 29.75$ MPa, $\lambda^\circ(\text{Cl}^-)$ derived using KCl transference numbers; *open diamond*, Ho et al. [21] $p = 29.75$ MPa, $\lambda^\circ(\text{Cl}^-)$ derived using NaCl transference numbers; *solid line*, Zimmerman et al. [28], $p = 20$ MPa; *dotted line*, Zimmerman et al. [28], $p = 29.75$ MPa

$p = 29.75$ MPa), and were corrected to $p = 29.75$ MPa, using viscosity data from NIST and assuming that Walden's rule is valid.

A comparison of these three sets of data provides a powerful means of estimating the accuracy and self-consistency of the linear extrapolation procedure since the values for NaCl and KCl are independent of one another. The two independent sets of values obtained for $\lambda^\circ(\text{Cl}^-)$ agree to within 2.5 %. This demonstrates that the results from the two extrapolation methods (Eqs. 9, 10) agree to within the combined experimental uncertainties of ± 1 % for each measurement, as defined by the precision of the duplicate measurements of $A^{\text{expt}}(\text{NaCl})$ at each temperature.

Our experimental values for $\lambda^\circ(\text{Cl}^-)$ can also be compared to the fitted equation recommended by Zimmerman et al. [28] from their critical evaluation of the literature data for NaCl, plotted as the solid curve in Fig. 4. The values for $\lambda^\circ(\text{Cl}^-)$ from Zimmerman et al.'s expression are greater than the results from our KCl and NaCl measurements, but agree to within 2.5 and 5 %, with the greatest variance observed at high temperature. The results for $\lambda^\circ(\text{Cl}^-)$ from the high temperature values for $A^\circ(\text{NaCl})$ and $A^\circ(\text{KCl})$ reported by Ho et al. [21] agree with one another to within 2 %, except near the critical point of water ($T = 673$ K) where the larger discrepancy may be attributed to a failure of Walden's rule to hold true or to larger experimental uncertainties at these conditions. These values are higher than the fitted expression from Zimmerman et al. [28] by 3 and 5 %, respectively.

We have chosen to use the values for $\lambda^\circ(\text{Cl}^-)$ from the transference numbers for KCl in H_2O , Eq. 10, to calculate single ion properties from the experimental results in Table 1.

These values were selected because they lie between the results for $\lambda^\circ(\text{Cl}^-)$ determined using $r^\circ(\text{NaCl})$ from this work and those from the critical compilation by Zimmerman et al. [28]. We assign them an uncertainty of $\pm 3\%$ in absolute accuracy, based on this comparison, and an uncertainty of $\pm 1\%$ in precision relative to the values of Λ° reported in Table 1. It is not possible to assess the accuracy of the values for $\lambda^\circ(\text{Cl}^-)$ in D_2O because there are no high temperature data with which to compare the assumptions used in deriving Eqs. 11 and 12. The precision relative to the values of Λ° for the salts reported in Table 2 is also $\pm 1\%$.

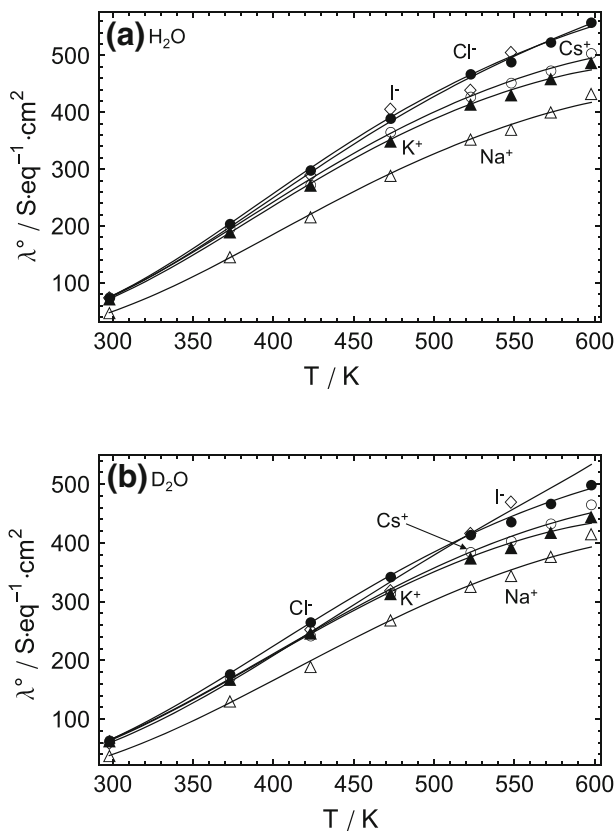
4.4 The Effect of Temperature on Limiting Conductivities of Univalent Cations

Single ion limiting conductivity data, λ° , for the cations Na^+ , K^+ and Cs^+ in light and heavy water were derived from the molar limiting conductivity data for the salts, Λ° , in Tables 1 and 2, by subtracting the contributions of $\lambda^\circ(\text{Cl}^-)$ according to Kohlrausch's law:

$$\lambda^\circ(\text{M}^+) = \Lambda^\circ(\text{M}^+\text{Cl}^-) - \lambda^\circ(\text{Cl}^-) \quad (13)$$

The resulting values of λ° for the cations in H_2O and in D_2O are tabulated in Tables 5 and 6, and plotted as a function of temperature in Fig. 5a, b, along with the values of $\lambda^\circ(\text{Cl}^-)$ from which they were derived. The tables include estimated uncertainty limits $\delta\lambda^\circ(\text{M}^+)$ calculated from the precisions of $\lambda^\circ(\text{Cl}^-)$ and $\Lambda^\circ(\text{MCl})$, according to the expression:

Fig. 5 Experimental single ion conductivity of aqueous univalent ions in **a** H_2O and **b** D_2O from $T = 298\text{--}600\text{ K}$ at $p = 20\text{ MPa}$: filled circle, Cl^- ; filled triangle, K^+ ; open triangle, Na^+ ; open diamond, I^- ; open circle, Cs^+ ; solid line, Eq. 17



$$\delta\lambda^\circ(\text{M}^+) = \left[\{\delta A^\circ(\text{M}^+\text{Cl}^-)\}^2 + \{\delta\lambda^\circ(\text{Cl}^-)\}^2 \right]^{1/2} \tag{14}$$

We note that these are uncertainties refer to relative precision rather than absolute accuracy. The values of λ° in both solvents follow the order $\text{Cl}^- > \text{Cs}^+ > \text{K}^+ > \text{Na}^+$ at all temperatures.

The only high temperature study with which to compare our results is that of Smolyakov and Veselova [61], who measured the limiting conductivity of the alkali metal chlorides from 178 to 473 K in H_2O at steam saturation pressure, p_{sat} . Their results for A° are consistent with the values in Tables 1 and 2. At 298.15 K their results, and the results from Refs. [30, 32], are ~2–5 % lower. The direction of these differences is consistent with the difference in viscosity between p_{sat} and $p = 20$ MPa, but the magnitude is greater.

While a number of empirical models [13, 14, 28, 62–66] have been proposed to describe the dependence of limiting molar or single ion conductivities on temperature and pressure (or density), only three apply to hydrothermal conditions. Oelkers and Helgeson [64, 65] used an approach based on Arrhenius energies of activation, similar to those of Brummer and Hills [62] and Smolyakov and Veselova [63], to predict the single ion limiting conductivities of a large number of ions for use in modeling geochemical systems. Marshall [13, 14] devised a “reduced state” relationship, based on a linear dependency of limiting single ion conductivity with density at constant temperature, relative to a hypothetical limit at zero density. More recently, Zimmerman et al. [28, 67, 68] reported that A° could be accurately represented by simple empirical functions of the solvent viscosity over a wide range of temperatures and pressures. We tested all of these equations and found that the best fit to the data in Tables 5 and 6 was obtained using the model by Zimmerman et al. [28], which takes the form:

$$\log_{10} \lambda^\circ = \log_{10} A_1 + \left(A_2 + \frac{A_3}{\rho_w} \right) \log_{10} \eta \tag{15}$$

Here, A_1 , A_2 , and A_3 are empirical fitting parameters, different for each ion, and ρ_w is the solvent density. The standard deviation in $\log_{10} \lambda^\circ$ of the fits were between 0.008 and 0.015, and values for the fitted parameters are listed in Table 7. The fit to the data for the

Table 7 Fitted parameters (Eqs. 15, 17) for single ion limiting conductivities for Cl^- , K^+ , Na^+ , Cs^+ and I^- ions in H_2O and D_2O

| Ion | Fit (Eq. 15) | | | Fit (Eq. 17) | | |
|------------------------------------|--------------------|--------------------|-------|-------------------|--------------------|------------------|
| | A_1 | A_2 | A_3 | a | $b \cdot R$ | $c \cdot R$ |
| $\text{Cl}^-/\text{H}_2\text{O}$ | 0.142 ± 0.052 | -0.851 ± 0.019 | 0 | 12.32 ± 1.51 | $-2,322 \pm 150$ | 320.5 ± 22.4 |
| $\text{Cl}^-/\text{D}_2\text{O}$ | 0.202 ± 0.055 | -0.826 ± 0.020 | 0 | 14.33 ± 1.41 | $-2,473 \pm 142$ | 337.2 ± 21.0 |
| $\text{K}^+/\text{H}_2\text{O}$ | -0.204 ± 0.055 | -0.926 ± 0.020 | 0 | 15.84 ± 2.27 | $-2,774 \pm 219$ | 383.0 ± 32.8 |
| $\text{K}^+/\text{D}_2\text{O}$ | -0.260 ± 0.067 | -0.950 ± 0.024 | 0 | 17.59 ± 1.85 | $-2,884 \pm 182$ | 393.4 ± 26.8 |
| $\text{Na}^+/\text{H}_2\text{O}$ | 0.214 ± 0.055 | -0.808 ± 0.020 | 0 | 10.27 ± 3.14 | $-2,717 \pm 325$ | 370.7 ± 48.6 |
| $\text{Na}^+/\text{D}_2\text{O}$ | 0.275 ± 0.057 | -0.786 ± 0.021 | 0 | 5.158 ± 5.863 | $-2,771 \pm 634$ | 375.5 ± 93.2 |
| $\text{Cs}^+/\text{H}_2\text{O}^a$ | 0.238 ± 0.055 | -0.805 ± 0.019 | 0 | 17.07 ± 3.81 | $-2,631 \pm 368$ | 362.5 ± 55.1 |
| $\text{Cs}^+/\text{D}_2\text{O}^a$ | 0.264 ± 0.037 | -0.793 ± 0.014 | 0 | 19.38 ± 3.31 | $-2,676 \pm 331$ | 363.1 ± 48.8 |
| $\text{I}^-/\text{H}_2\text{O}$ | 0.071 ± 0.077 | -0.878 ± 0.028 | 0 | 15.21 ± 27.77 | $-2,132 \pm 2,870$ | 291.2 ± 431 |
| $\text{I}^-/\text{D}_2\text{O}$ | 0.018 ± 0.042 | -0.894 ± 0.016 | 0 | 19.25 ± 22.41 | $-1,739 \pm 2,416$ | 228.1 ± 357 |

^a Values of $\lambda^\circ(\text{Cs}^+)$ used in the fits to Eqs. 15 and 17 were obtained from $A^\circ(\text{CsCl})$ except at $T = (298, 423$ and $473)$ K where they were taken from $A^\circ(\text{CsI})$

iodide ion had a larger standard deviation in $\log_{10} \lambda^\circ$ of 0.019. None of the models could reproduce the small inflection point at ~ 550 K, with the result that all showed a systematic deviation of +5 % or more between experimental data and fitted results somewhere in the range 350–500 K.

An improved fit was obtained from an empirical fitting equation that we derived from a relationship reported by Smolyakov and Veselova [63]:

$$\log_{10} \lambda^\circ \eta = A + \frac{E_\eta - E_{\lambda^\circ}}{RT}, \quad (16)$$

where E_η is the activation energy of viscosity and E_{λ° is the activation energy of ionic conductance. The new fitting expression takes the form:

$$\log_{10} \lambda^\circ \eta = \frac{a}{T - 228} + \frac{b + c \ln \rho_w}{RT}, \quad (17)$$

where ρ_w is the density of water or heavy water. The pre-exponential factor, $A = a/(T - 228)$, was chosen to yield a discontinuity at $T = 228$ K. This is the temperature usually associated with the critical point between the high and low density forms of the liquid in super-cooled water [43, 69–71], and it is intended to reproduce the strong temperature dependence of “structure-making” and “structure-breaking” effects at sub-ambient temperatures, described in the following section. The critical point in super-cooled D₂O is thought to be at $T = (230 \pm 5)$ K [72], consistent with Eq. 17, to within the margin of error. The Arrhenius energy term, $[E_\eta - E_{\lambda^\circ}] = b + c \ln \rho_w$, was taken from the expression for the standard molar internal energy of reaction from the “density” model of [73], which describes the solvent compressibility effects on chemical equilibria at elevated temperatures and pressures [74].

The standard deviations in $\log_{10} \lambda^\circ \eta$ of the fits were between 0.004 and 0.008 for ions in H₂O and between 0.004 and 0.014 for ions in D₂O. Values for the fitted parameters are listed in Table 7. The fits of Eq. 17 to the data for the iodide ion had a larger standard deviation in $\log_{10} \lambda^\circ \eta$ of 0.016 (H₂O) and 0.012 (D₂O). This was the only ion for which three parameter fits were not statistically significant. We were unable to identify a reason for the visibly larger statistical scatter in the results for $\lambda^\circ(\text{I}^-)$, but suspect it may arise from sorption effects or redox reactions with the platinum surfaces in the cell. Finally we note that Eq. 17 yielded statistically superior fits for our values of λ° relative to those obtained from Eq. 15. We recommend its use to represent the behaviour of λ° over a wide range of density and temperature.

5 Discussion

5.1 Temperature Dependence of Limiting Conductivities

The classical interpretation of ionic conductivities is based on the model by Frank and Wen [75] for ionic hydration, which is summarized in the review paper by Kay [76]. Briefly, the effects of temperature on limiting conductivities can be discussed in terms of the Walden product $\lambda^\circ \eta$. The Walden product is related to the “effective” ionic radius r_{Stokes} through Stokes law,

$$\lambda^\circ \eta = \frac{Fz_i e}{\pi f r_{\text{Stokes}}}, \quad (18)$$

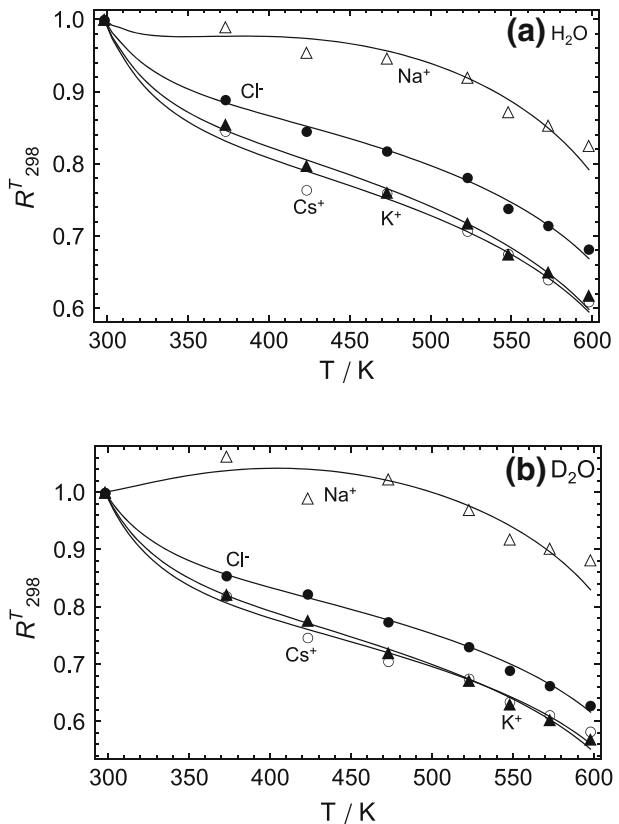
in which $6 \geq f \geq 4$ is a boundary factor ranging between perfect slip and perfect sticking, and $e \cdot z_i$ is the ionic charge. Stokes' law does not adequately describe limiting conductivities because it ignores ion–solvent, and solvent–solvent interactions at the molecular level [77]. More sophisticated continuum models such as the Hubbard–Onsager theory [78, 79] are only partly successful in describing these effects. The Frank–Wen model for ionic hydration [75] postulates that the perturbations of an ion on the hydrogen-bonding of bulk water can be inferred from the temperature dependence of the Walden product ratio,

$$R_{298}^T = \frac{(\lambda^\circ \eta_w)_T}{(\lambda^\circ \eta_w)_{T=298K}} \tag{19}$$

In this model, the so-called “structure-making” ions are defined as those with $R_{298}^T > 1$ and “structure-breaking” ions are those with $R_{298}^T < 1$. A modern interpretation of this classification that includes thermodynamic transfer properties and spectroscopic results is given by Marcus [80].

Figure 6 presents plots of the Walden product ratio R_{298}^T for the chloride ion and the cations Na^+ , K^+ and Cs^+ in H_2O and D_2O , relative to their values at 298.15 K, based on values for the limiting single ion conductivities in Table 5. The trends in R_{298}^T for the two solvents are very similar, and the discussion that follows in this section will focus on temperature-dependent ionic hydration effects in light water. The iodide ion was not

Fig. 6 Temperature dependence of the Walden product ratio $\{(\lambda^\circ \eta)_T / (\lambda^\circ \eta)_{298.15K}\}$ for aqueous univalent ions in **a** H_2O and **b** D_2O from $T = 298\text{--}600$ K at $p = 20$ MPa: filled circle, Cl^- ; filled triangle, K^+ ; open triangle, Na^+ ; open diamond, I^- ; open circle, Cs^+ ; solid line, Eq. 17



included in this analysis because of the larger uncertainty limits noted above. We note that only Eq. 17 is able to reproduce the two inflection points observed in Fig. 6. Based on Kay's interpretation of the values of R_{298}^T near ambient conditions and Marcus' classification, Na^+ is considered to be a borderline ion with a strongly-bound first hydration shell and a largely temperature-dependent Walden product. In both the classical and modern descriptions, K^+ and Cs^+ are classified as "structure-breakers" at ambient conditions. These are large cations with a lower surface charge density and less tightly bound first hydration spheres that disrupt the three dimensional hydrogen-bonding in water and lower the local viscosity. The Cl^- anion is also a "structure-breaker" with a loosely-bound first hydration sphere which provides excess mobility at temperatures below 298 K.

These "structure-making" and "structure breaking" effects decrease with increasing temperature as the nature of the ion–water interactions changes. As the temperature is raised from ambient conditions towards the critical point [81] (H_2O : $T_c = 647.10$ K, $p_c = 22.06$ MPa, $\rho_c = 0.322$ g·cm⁻³; D_2O : $T_c = 643.85$ K, $p_c = 21.67$ MPa, $\rho_c = 0.356$ g·cm⁻³), the hydrogen bonded coordination number decreases from ~ 4 to ~ 2 , and the isothermal compressibility becomes very large [82]. At temperatures above ~ 400 K, the dominant effect is the long-range polarization of the bulk solvent due to charge–dipole interactions with liquid water, as described by the classical Born equation. These effects are reflected in the standard partial molar volumes of aqueous ions which rise to a maximum at ~ 330 to 360 K as short-range hydration effects become less important, then decrease towards large negative values at the critical point due to the electrostriction caused by long-range solvent polarization [74, 83]. As a result, the Walden product ratio, expressed by Eq. 19, would be expected to decrease with increasing temperature due to the viscous drag associated with a more densely packed "hydration" sphere of oriented solvent molecules around each of the ions. These effects have been quantified by Xiao and Wood [84], who used a compressible continuum model to describe the effects of electrostriction and electroviscosity on ionic transport in high temperature water. Their model correctly predicts (i) that Walden's rule is not obeyed, (ii) that the limiting conductivities λ° are a strong function of density, and a very weak function of temperature at constant density, and (iii) that the values of λ° for small ions converge towards similar values under near-critical conditions where compressibility effects are large.

The plots of R_{298}^T in Fig. 6 are consistent with this qualitative description, and with the compressible continuum models of Xiao and Wood. The Walden product of Na^+ at 600 K is lower than its value at 298 K by about 15 %, while those of K^+ and Cs^+ are lower by ~ 40 %, reflecting the more tightly bound first hydration sphere of Na^+ and the larger effective radius of the hydrated ion. The behavior of the chloride ion is intermediate between these two results.

We note that these descriptions of ionic hydration effects from classical models are supported by molecular dynamics simulations, such as those of Balbuena et al. [85] who confirmed that the strongly bound first shell of both cations and anions persists well into the high-temperature, low density range of supercritical water. Their simulation showed that coordination number for cations decreases with increasing temperature, while the coordination number for anions increases. As an example, for Na^+ the number of water molecules in the first hydration sphere decreased from $n_w = 5.2$ at 298 K to $n_w = 4.5$ at 673 K, while those for Cl^- increased from $n_w = 7.4$ to $n_w = 8.1$. Moreover, the simulations confirmed the increasing importance of long-range solvent polarization to ionic hydration in dense, near-critical water, as described by semi-continuum models based on the Born equation [43, 86] and the "density" model [74]. A more complete review is given by Seward and Driesner [87] and Driesner [88].

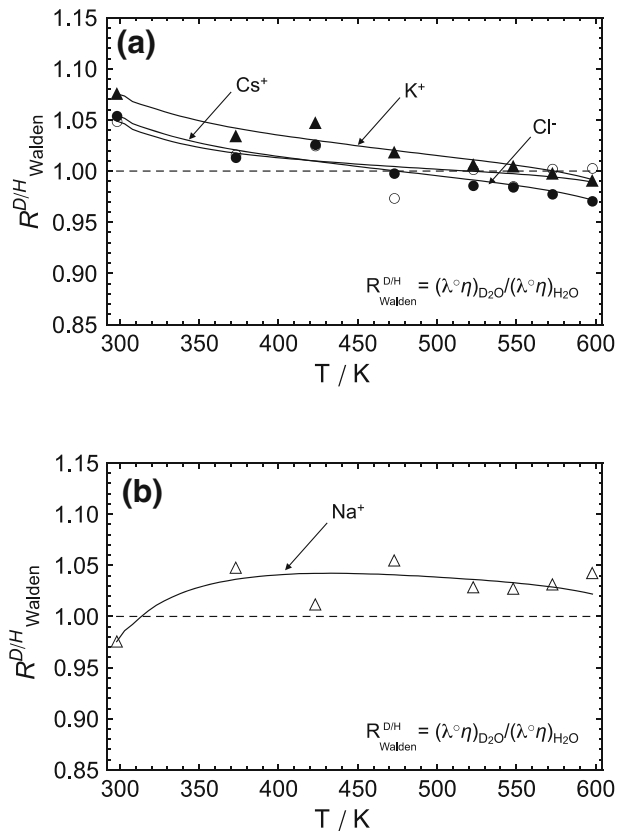
5.2 Deuterium Isotope Effects

Although Stokes’ law equates the Walden product $\lambda^\circ \eta_w$ with the “effective” ionic radius, the compressible continuum ionic transport model [84] and modern interpretations of experimental data [77] show that this interpretation is not valid at the conditions relevant to the present study. An alternative approach, initiated by Swain and Evans [30] and also pursued by Broadwater and Evans [31, 32] and Tada et al. [33–35] is to use the isotopic ratio of the Walden product in heavy and light water, $(\lambda^\circ \eta)_{D_2O}/(\lambda^\circ \eta)_{H_2O}$, as a means of examining *relative* differences in ionic hydration between the two solvents. We have adopted the Swain–Evans approach, as a practical tool to quantify and interpret the deuterium isotope effect on single-ion limiting conductivities. Values for the isotopic Walden product ratio:

$$R_{\text{Walden}}^{\text{D/H}} = \frac{(\lambda^\circ \eta)_{D_2O}}{(\lambda^\circ \eta)_{H_2O}} = \frac{r_{\text{Stokes-H}_2\text{O}}}{r_{\text{Stokes-D}_2\text{O}}}, \tag{20}$$

for the chloride ion and the cations, were calculated from the limiting single-ion conductivities in Tables 5 and 6, and the physical property data in Table 4. These are plotted in Fig. 7a, b, along with the values of $R_{\text{Walden}}^{\text{D/H}}$ calculated from Eq. 20, using the fitted parameters listed in Table 7. The interpretation of these plots has been described by Swain

Fig. 7 a Isotopic Walden product ratio, $R_{\text{Walden}}^{\text{D/H}}$, of aqueous chloride, potassium and cesium ions from $T = 298\text{--}598\text{ K}$ at $p = 20\text{ MPa}$: filled circle, Cl^- ; filled triangle, K^+ ; open circle, Cs^+ ; solid line, Eq. 17. **b** Isotopic Walden product ratio, $R_{\text{Walden}}^{\text{D/H}}$, of aqueous sodium ion from $T = 298\text{--}598\text{ K}$ at $p = 20\text{ MPa}$: open triangle, Na^+ ; solid line, Eq. 17



and Evans [30], Broadwater and Kay [32], and Broadwater and Evans [31], based on the stronger hydrogen bonding in D_2O relative to H_2O . In their treatment, values of $R_{Walden}^{D/H}$ equal to unity indicate that the efficiency of ionic transport mechanism is the same in both solvents, while values $R_{Walden}^{D/H} > 1$ indicate that the ions diffuse more readily in heavy water, consistent with “structure breaking” behavior. Values of $R_{Walden}^{D/H} < 1$ indicate a more efficient transport mechanism in light water, and are interpreted as being due to “structure making” ions. We note that the limiting conductivities at 298.15 K at $p = 20$ MPa, in both H_2O and D_2O , are larger than those in Refs. [30–32], which were measured at $p = 0.1$ MPa.

As shown in Fig. 7a, the isotopic Walden product ratio for the chloride ion at 298.15 K is greater than unity, $R_{Walden}^{D/H}(Cl^-) = 1.05 \pm 0.02$, consistent with its classification of it as a “structure breaker” under ambient conditions [30–32, 76, 89]. This value decreases to unity at ~ 473 K, then continues to fall to $R_{Walden}^{D/H}(Cl^-) = 0.97 \pm 0.02$, indicating that the deuterium isotope effect is negligible at this temperature, to within the experimental uncertainties. Likewise, the values for potassium and cesium, $R_{Walden}^{D/H}(K^+) = 1.07 \pm 0.02$ and $R_{Walden}^{D/H}(Cs^+) = 1.05 \pm 0.02$, are consistent with their classification as “structure” breakers at room temperature. Like chloride, these values fall to unity at elevated temperatures, $R_{Walden}^{D/H} = 0.99 \pm 0.02$ and 1.00 ± 0.02 at 600 K. The sodium ion is considered to be a borderline “structure maker” [30–32, 76, 89] and its value at 298.15 K, $R_{Walden}^{D/H}(Na^+) = 0.98 \pm 0.02$, reflects this assessment. This value rises above unity to approximately constant values of $\sim 1.04 \pm 0.02$ at temperatures above ~ 375 K (see Fig. 7b). Here and for each of the ions discussed above, the uncertainty is taken to be the 95 % confidence limit for the values of $R_{Walden}^{D/H}$ above 370 K, relative to their mean value. A decrease in $R_{Walden}^{D/H}$ toward values below unity would be expected from ion–solvent polarization arguments because the critical temperature of D_2O is lower than that of H_2O . However, the departure from unity for the structure breaking ions is at the edge of being statistically significant. The decrease in $R_{Walden}^{D/H}(Na^+)$ between 370 and 600 K is not statistically significant, suggesting that there may be a deuterium isotope effect on $\lambda^\circ(Na^+)$ at sub-critical conditions that persists at higher temperatures but that the effect is small.

6 Conclusions

This paper reports the first measurements of accurate electrical conductivities of aqueous salts in D_2O under hydrothermal conditions. By using a high-precision flow-through AC electrical conductance instrument, it was possible to make measurements of similar nearly identical solutions in heavy and light water in sequence, so that many of the systematic errors associated with high temperature conductivity measurements cancel one another. The values for $\lambda^\circ(Cl^-)$ in H_2O and D_2O obtained from this method appear to be precise to within ± 1 %. The principal uncertainty is in the systematic uncertainty associated with extrapolation of transference numbers for NaCl and KCl in D_2O . The determination of $\lambda^\circ(Cl^-)$ is an important result because it defines a single-ion conductivity scale for electrolyte solutions in heavy water for the first time. These self-consistent values of $\lambda^\circ(Cl^-)$ were used to calculate the single ion limiting conductivities of three alkali metal cations, which follow the order $\lambda^\circ(Na^+) < \lambda^\circ(K^+) \leq \lambda^\circ(Cs^+) < \lambda^\circ(Cl^-)$ at all temperatures in both

light and heavy water. The Walden product ratio of all these ions drops dramatically with increasing temperature, in the order $R_{298}^T(\text{Na}^+) < R_{298}^T(\text{Cl}^-) < R_{298}^T(\text{K}^+) \approx R_{298}^T(\text{Cs}^+)$, reflecting the shift towards hydration effects associated with long-range solvent polarization. The temperature dependence of the isotopic Walden product ratio, $(\lambda^\circ\eta)_{\text{D}_2\text{O}}/(\lambda^\circ\eta)_{\text{H}_2\text{O}}$ indicates that differences in the hydration of Cl^- , K^+ and Cs^+ between light and heavy water at ambient conditions associated with hydrogen-bonding, the so-called “structure breaking” effects, largely disappear at temperatures above ~ 400 K. The value of $(\lambda^\circ\eta)_{\text{D}_2\text{O}}/(\lambda^\circ\eta)_{\text{H}_2\text{O}}$ for the “structure making” ion Na^+ rises from 0.98 at 298.15 K to $\sim 1.04 \pm 0.02$ at temperatures above ~ 375 K and remains approximately constant up to 600 K. These changes are consistent with the onset of long-range ion-solvent polarization as the dominant hydration effect as the critical temperature is approached.

7 Supplementary Material

The experimental limiting conductivities of $\text{NaCl}(\text{aq})$ from this current work, earlier papers, and the recent model reported by Zimmerman [22] are plotted in Fig. S1, which is included in the electronic supplementary material.

Acknowledgments The authors express their deep gratitude to Prof. Robert H. Wood, University of Delaware, for donating the AC conductance cell to the Hydrothermal Chemistry Laboratory at the University of Guelph. We are grateful to both Professor Wood and Professor Greg Zimmerman for providing us with the benefit of their extensive operating experience, and for many fruitful discussions. We also thank Mr. Ian Renaud and Mr. Casey Gielen of the electronics shop and machine shop in the College of Physical and Engineering Science at the University of Guelph for their very considerable expertise in maintaining and modifying the instrument and its data acquisition system. This research was supported by the Natural Science and Engineering Research Council of Canada (NSERC), Ontario Power Generation Ltd. (OPG), and the University Network of Excellence in Nuclear Engineering (UNENE). Technical advice and encouragement were provided by Dr. Dave Guzonas, Atomic Energy of Canada Ltd.; Dr. Dave Evans, Ontario Power Generation Ltd.; and Dr. Mike Upton, Bruce Power Ltd.

References

1. Weingärtner, H., Franck, E.U.: Supercritical water as a solvent. *Angew. Chem. Int. Ed.* **44**, 2672–2692 (2005)
2. Corti, H.R., Trevani, L.N., Anderko, A.: Transport properties in high temperature and pressure ionic solutions. In: Palmer, D.A., Fernández-Prini, R., Harvey, A.H. (eds.) *Aqueous Systems at Elevated Temperatures and Pressures: Physical Chemistry in Water, Steam and Aqueous Solutions*, Chap. 10, pp. 321–376. Elsevier Academic Press, New York (2004)
3. Frantz, J.D., Marshall, L.: Electrical conductances and ionization constants of salts, acids, and bases in supercritical aqueous fluids: I. Hydrochloric acid from 100° to 700 °C and at pressures to 4000 bars. *Am. J. Sci.* **284**, 651–667 (1984)
4. Marshall, W.L., Frantz, J.D.: Electrical conductance measurements of dilute, aqueous electrolytes at temperatures up to 800 °C and pressures to 4264 bars: techniques and interpretations. In: Ulmer, G.C., Barnes, H.L. (eds.) *Hydrothermal Experimental Techniques*, pp. 216–292. Wiley-Interscience Publication, New York (1987)
5. Noyes, A.A., Coolidge, W.D.: The electrical conductivity of aqueous solutions at high temperatures, I. Description of the apparatus. Results with NaCl and KCl up to 306 °C. *Z. Phys. Chem.* **46**, 323–378 (1904)
6. Noyes, A.A., Coolidge, W.D.: The electrical conductivity of aqueous solutions at high temperatures. *J. Am. Chem. Soc.* **26**, 134–170 (1904)
7. Noyes, A.A., Melcher, A.C., Cooper, H.C., Eastman, G.W., Kato, Y.: The conductivity and ionization of salts, acids, and bases in aqueous solutions at high temperatures. *J. Am. Chem. Soc.* **30**, 335–353 (1908)

8. Noyes, A.A., Melcher, A.C., Cooper, H.C., Eastman, G.W.: The conductivity and ionization of salts, acids, and bases in aqueous solutions at high temperatures. *Z. Phys. Chem.* **70**, 335–377 (1910)
9. Franck, E.U.: Hochverdichteter Wasserdampf III. Ionizen dissoziation von HCl, KOH und H₂O in Ueberkritischem Wasser, 2. *Z. Phys. Chem.* **8**, 192–206 (1956)
10. Quist, A.S., Marshall, W.L.: Assignment of limiting equivalent conductances for single ions to 400°. *J. Phys. Chem.* **69**, 2984–2987 (1965)
11. Quist, A.S., Marshall, W.L.: Electrical conductances of aqueous sodium chloride solutions from 0 to 800° and at pressures to 4000 bar. *J. Phys. Chem.* **72**, 684–703 (1968)
12. Horvath, A.L.: *Handbook of Aqueous Electrolyte Solutions: Physical Properties, Estimation and Correlation Methods*, pp. 249–284. Ellis Horwood Ltd., Chichester (1985)
13. Marshall, W.L.: Reduced state relationship for limiting electrical conductances of aqueous ions over wide ranges of temperature and pressure. *J. Chem. Phys.* **87**, 3639–3643 (1987)
14. Marshall, W.M.: Electrical conductance of liquid and supercritical water evaluated from 0 °C and 0.1 MPa to high temperatures and pressures: reduced-state relationships. *J. Chem. Eng. Data* **32**, 221–226 (1987)
15. Smith, J.E., Dismukes, E.B.: Transference numbers in aqueous sodium chloride at elevated temperatures. *J. Phys. Chem.* **68**, 1603–1606 (1964)
16. Ho, P.C., Palmer, D.A., Mesmer, R.E.: Electrical conductivity measurements of aqueous sodium chloride solutions to 600 °C and 300 MPa. *J. Solution Chem.* **23**, 997–1018 (1994)
17. Bianchi, H., Corti, H.R., Fernández-Prini, R.: Electrical conductivity of aqueous sodium hydroxide solutions at high temperatures. *J. Solution Chem.* **23**, 1203–12012 (1994)
18. Zimmerman, G.H., Gruskiewicz, M.S., Wood, R.H.: New apparatus for conductance measurements at high temperatures: conductance of aqueous solutions of LiCl, NaCl, NaBr, and CsBr at 28 MPa and water densities from 700 to 260 kg m⁻³. *J. Phys. Chem.* **99**, 11612–11625 (1995)
19. Sharygin, A.V., Wood, R.H., Zimmerman, G.H., Balashov, V.N.: Multiple ion association versus re-dissociation in aqueous NaCl and KCl at high temperatures. *J. Phys. Chem. B* **106**, 7121–7134 (2002)
20. Hnedkovsky, L., Wood, R.H., Balashov, V.N.: Electrical conductances of aqueous Na₂SO₄, H₂SO₄, and their mixtures: limiting equivalent ion conductances, dissociation constants, and speciation to 673 K and 28 MPa. *J. Phys. Chem. B* **109**, 9034–9046 (2005)
21. Ho, P.C., Bianchi, H., Palmer, D.A., Wood, R.H.: Conductivity of dilute aqueous electrolyte solutions at high temperatures and pressures using a flow cell. *J. Solution Chem.* **29**, 217–235 (2000)
22. Ho, P.C., Palmer, D.A., Wood, R.H.: Conductivity measurements of dilute aqueous LiOH, NaOH, and KOH solutions to high temperatures and pressures using a flow-through cell. *J. Phys. Chem. B* **104**, 12084–12089 (2000)
23. Ho, P.C., Palmer, D.A., Gruskiewicz, M.S.: Conductivity measurements of dilute aqueous HCl solutions to high temperatures and pressures using a flow-through cell. *J. Phys. Chem. B* **105**, 1260–1266 (2001)
24. Sharygin, A.V., Mokbel, I., Xiao, C., Wood, R.H.: Tests of equations for the electrical conductance of electrolyte mixtures: measurements of association of NaCl(aq) and Na₂SO₄(aq) at high temperatures. *J. Phys. Chem. B* **105**, 229–237 (2001)
25. Sharygin, A.V., Grafton, B.K., Xiao, C., Wood, R.H., Balashov, V.N.: Dissociation constants and speciation in aqueous Li₂SO₄ and K₂SO₄ from measurements of electrical conductance to 673 K and 29 MPa. *Geochim. Cosmochim. Acta* **70**, 5169–5182 (2006)
26. Zimmerman, G.H., Wood, R.H.: Conductance of dilute sodium acetate solutions to 469 K and of acetic acid and sodium acetate/acetic acid mixtures to 548 K and 20 MPa. *J. Solution Chem.* **31**, 995–1017 (2002)
27. Méndez De Leo, L.P., Wood, R.H.: Conductance study of association in aqueous CaCl₂, Ca(CH₃COO)₂, and Ca(CH₃COO)₂*n*CH₃COOH from 348 to 523 K at 10 MPa. *J. Phys. Chem. B* **109**, 14243–14250 (2005)
28. Zimmerman, G.H., Arcis, H., Tremaine, P.R.: Limiting conductivities and ion association constants of aqueous NaCl under hydrothermal conditions: experimental data and correlations. *J. Chem. Eng. Data* **57**, 2415–2429 (2012)
29. Zimmerman, G.H., Arcis, H., Tremaine, P.R.: Limiting conductivities and ion association in aqueous NaCF₃SO₃ and Sr(CF₃SO₃)₂ from 298 to 623 K at 20 MPa. Is triflate a non-complexing anion in high temperature water? *J. Chem. Eng. Data* **57**, 3180–3197 (2012)
30. Swain, C.G., Evans, D.F.: Conductance of ions in light and heavy water at 25°. *J. Am. Chem. Soc.* **88**, 383–390 (1966)
31. Broadwater, T.L., Evans, D.F.: The conductance of divalent ions in H₂O at 10 and 25 °C and in D₂O. *J. Solution Chem.* **3**, 757–769 (1974)

32. Broadwater, T.L., Kay, R.L.: The temperature coefficient of conductance for the alkali metal, halide, tetraalkylammonium, halate, and perchlorate ions in D₂O. *J. Solution Chem.* **4**, 745–762 (1975)
33. Tada, Y., Ueno, M., Tsuchihashi, N., Shimizu, K.: Pressure and temperature effects on the excess deuterium and proton conductance. *J. Solution Chem.* **21**, 971–985 (1992)
34. Tada, Y., Ueno, M., Tsuchihashi, N., Shimizu, K.: Pressure and isotope effects on the proton jump of the hydroxide ion at 25 °C. *J. Solution Chem.* **22**, 1135–1149 (1993)
35. Tada, Y., Ueno, M., Tsuchihashi, N., Shimizu, K.: Comparison of temperature, pressure and isotope effects on the proton jump between the hydroxide and oxonium ion. *J. Solution Chem.* **23**, 973–987 (1994)
36. Guzonas, D., Brosseau, F., Tremaine, P., Meesungnoen, J., Jay-Gerin, J.-P.: Key water chemistry issues in a supercritical-water-cooled pressure-tube reactor. *Nucl. Technol.* **179**, 205–279 (2012)
37. Erickson, K.M., Arcis, H., Raffa, D., Zimmerman, G.H., Tremaine, P.R.: Deuterium isotope effects on the ionization constant of acetic acid in H₂O and D₂O by AC conductance from 100 C to 275 C at 20 MPa. *J. Phys. Chem B* **115**, 3038–3151 (2011); erratum: Erickson, K.M., Arcis, H., Raffa, D., Zimmerman, G.H., Tremaine, P.R.: *J. Phys. Chem B* (in preparation)
38. Arcis, H., Zimmerman, G.H., Tremaine, P.R.: Ion-pair formation in aqueous strontium chloride and strontium hydroxide solutions under hydrothermal conditions by AC conductivity measurements. *Phys. Chem. Chem. Phys.* **16**, 17688–17704 (2014)
39. Hamann, S.D., Linton, M.: Influence of pressure on the rates of deuterium of formate and acetate ions in liquid D₂O. *Aust. J. Chem.* **30**, 1883–1889 (1977)
40. Zimmerman, G.H., Arcis, H.: Extrapolation methods for AC impedance measurements made with a concentric cylinder cell on solutions of high ionic strength. *J. Solution Chem.* (2014). doi:[10.1007/s10953-014-0208-x](https://doi.org/10.1007/s10953-014-0208-x)
41. Barthel, J., Feuerlein, F., Neuder, R., Wachter, R.: Calibration of conductance cells at various temperatures. *J. Solution Chem.* **9**, 209–219 (1980)
42. Helgeson, H.C., Kirkham, D.H., Flowers, G.C.: Theoretical prediction of the thermodynamic behavior of aqueous electrolytes at high pressures and temperatures. IV. Calculation of activity coefficients, osmotic coefficients, and apparent molal and standard and relative partial molal properties to 600 °C and 5 Kbar. *Am. J. Sci.* **281**, 1249–1516 (1981)
43. Tanger IV, J.C., Helgeson, H.C.: Calculation of the thermodynamic and transport properties of aqueous species at high pressures and temperatures: revised equations of state for the standard partial molal properties of ions and electrolytes. *Am. J. Sci.* **288**, 19–98 (1988)
44. Shock, E.L., Helgeson, H.C.: Calculation of the thermodynamic and transport properties of aqueous species at high pressures and temperatures: correlation algorithms for ionic species and equation of state predictions to 5 kb and 1000 °C. *Geochim. Cosmochim. Acta* **52**, 2009–2036 (1988)
45. Johnson, J.W., Oelkers, E.H., Helgeson, H.C.: SUPCRT92: a software package for calculating the standard molal thermodynamic properties of minerals, gases, aqueous species, and reactions from 1 to 5000 bar and 0 to 1000 °C. *Comput. Geosci.* **18**, 899–947 (1992)
46. Wagner, W., Pruss, A.: The IAPWS formulation 1995 for the thermodynamic properties of ordinary water substance for general and scientific use. *J. Phys. Chem. Ref. Data* **31**, 387–535 (2002)
47. Fernandez, D.P., Goodwin, A.R.H., Lemmon, E.W., Levelt-Sengers, J.M.H., Williams, R.C.: A formulation for the static permittivity of water and steam at temperatures from 238 K to 873 K at pressures up to 1200 MPa, including derivatives and Debye–Hückel coefficients. *J. Phys. Chem. Ref. Data* **26**, 1125–1166 (1997)
48. Hill, P.G., MacMillan, R.D.C., Lee, V.A.: Fundamental equation of state for heavy water. *J. Phys. Chem. Ref. Data* **11**, 1–14 (1982)
49. “ASME and IAPWS Formulation for Water and Steam”, NIST Standard Ref. Database 10, 2.2; “REFPROP: Equations of State for Pure and Binary Fluids” NIST Standard Ref. Database 22, 8.0
50. Trevani, L.N., Balodis, E., Tremaine, P.R.: Apparent and standard partial molar volumes of NaCl, NaOH, and HCl in water and heavy water at $T = 523$ K and 573 K at $p = 14$ MPa. *J. Phys. Chem. B* **111**, 2015–2024 (2007)
51. Fernández-Prini, R.: Conductance of electrolyte solutions a modified expression for its concentration dependence. *Trans. Faraday Soc.* **65**, 3311–3313 (1969)
52. Bianchi, H., Dujovne, I., Fernández-Prini, R.: Comparison of electrolytic conductivity theories: performance of classical and new theories. *J. Solution Chem.* **29**, 237–253 (2000)
53. Longworth, L.G.: Transference numbers of aqueous solutions of potassium chloride, sodium chloride, lithium chloride and hydrochloric acid at 25° by the moving boundary method. *J. Am. Chem. Soc.* **54**, 2741–2758 (1932)
54. MacInnes, D.A., Longworth, L.G.: Transference numbers by the method of moving boundaries. *Chem. Rev.* **11**(2), 171–230 (1932)

55. Allgood, R.W., Le Roy, D.J., Gordon, A.R.: The variation of the transference numbers of potassium chloride in aqueous solution with temperature. *J. Chem. Phys.* **8**, 418–422 (1940)
56. Allgood, R.W., Gordon, A.R.: The variation of the transference numbers of sodium chloride in aqueous solution with temperature. II. *J. Chem. Phys.* **10**, 124–126 (1942)
57. Smith, J.E., Dismukes, E.B.: The cation transference number in aqueous potassium chloride at 70 to 115°. *J. Phys. Chem.* **67**, 1160–1161 (1963)
58. Ueno, M., Yoneda, A., Tsuchihashi, N., Shimizu, K.: Solvent isotope effect on mobilities of potassium and chloride ions in water at high pressure. II. A low temperature study. *J. Chem. Phys.* **86**, 4678–4683 (1987)
59. Nakahara, M., Zenke, M., Ueno, M., Shimizu, K.: Solvent isotope effect on ion mobility in water at high pressure: conductance and transference number of potassium chloride in compressed heavy water. *J. Chem. Phys.* **83**, 280–287 (1985)
60. Ueno, M., Tsuchihashi, N., Shimizu, K.: Solvent isotope effects on mobilities of potassium and chloride ion in water at high pressure. III. A high temperature study. *J. Chem. Phys.* **92**, 2548–2552 (1990)
61. Smolyakov, B.S., Veselova, G.A.: Limiting equivalent conductivity of Li^+ , Na^+ , K^+ , Rb^+ , Cs^+ and Cl^- ions in water at temperatures between 5 and 200 °C. I. Experimental data. *Sov. Electrochem.* **10**, 851–855 (1974)
62. Brummer, S.B., Hills, G.J.: Kinetics of ionic conductance. *Trans. Faraday Soc.* **57**, 1816–1837 (1961)
63. Smolyakov, B.S., Veselova, G.A.: Limiting equivalent conductivity of aqueous solutions of Li^+ , Na^+ , K^+ , Rb^+ , Cs^+ and Cl^- ions in water at temperatures between 5 and 200 °C. II. Relations between the limiting conductivity and the viscosity of water. *Sov. Electrochem.* **11**, 653–656 (1975)
64. Oelkers, E.H., Helgeson, H.C.: Calculation of the thermodynamic and transport properties of aqueous species at high pressures and temperatures: dissociation constants for supercritical alkali metal halides at temperatures from 400 to 800 °C and pressures from 500 to 4000 bar. *J. Phys. Chem.* **92**, 1631–1639 (1988)
65. Oelkers, E.H., Helgeson, H.C.: Calculation of the transport properties of aqueous species at pressures to 5 KB and temperatures to 1000 °C. *J. Solution Chem.* **18**, 601–640 (1989)
66. Longinotti, M.P., Corti, H.R.: Fractional Walden rule for electrolytes in supercooled disaccharide aqueous solutions. *J. Phys. Chem. B* **113**, 5500–5507 (2009)
67. Zimmerman, G.H., Scott, P.W., Greynolds, W.A.: New flow instrument for conductance measurements at elevated temperatures and pressures: measurements on NaCl(aq) to 458 K and 1.4 MPa. *J. Solution Chem.* **36**, 767–786 (2007)
68. Zimmerman, G.H., Scott, P.W., Greynolds, W., Mayorov, D.: Conductance of dilute hydrochloric acid solutions to 458 K and 1.4 MPa. *J. Solution Chem.* **38**, 499–512 (2009)
69. Holtén, V., Anisimov, M.A.: Entropy-driven liquid–liquid separation in supercooled water. *Sci. Rep.* **2**, 1–7 (2012)
70. Debenedetti, P.G.: Supercooled and glassy water. *J. Phys. Condens. Matter* **15**, R1669–R1726 (2003)
71. Mishima, O., Stanley, H.E.: The relationship between liquid, supercooled and glassy water. *Nature* **396**, 329–335 (1998)
72. Mishima, O.: Liquid–liquid critical point in heavy water. *Phys. Chem. Rev.* **85**, 334–336 (2000)
73. Anderson, G.M., Castet, S., Schott, J., Mesmer, R.E.: The density model for estimation of thermodynamic parameters of reactions at high temperatures and pressures. *Geochim. Cosmochim. Acta* **55**, 1769–1779 (1991)
74. Mesmer, R.E., Marshall, W.L., Palmer, D.A., Simonson, J.M., Holmes, H.F.: Thermodynamics of aqueous association and ionization reactions at high temperatures and pressures. *J. Solution Chem.* **17**, 699–718 (1988)
75. Frank, H.S., Wen, W.Y.: III Ion-solvent interaction structural aspects of ion–solvent interaction in aqueous solutions: a suggested picture of water structure. *Discuss. Faraday Soc.* **24**, 133–140 (1957)
76. Kay, R.L.: The current state of our understanding of ionic mobilities. *Pure Appl. Chem.* **63**, 1393–1399 (1991)
77. Marcus, Y.: Are ionic Stokes radii of any use? *J. Solution Chem.* **41**, 2082–2090 (2012)
78. Hubbard, J., Onsager, L.: Dielectric dispersion and dielectric friction in electrolyte solutions. I. *J. Chem. Phys.* **67**, 4850–4857 (1977)
79. Hubbard, J.: Dielectric dispersion and dielectric friction in electrolyte solutions. II. *J. Chem. Phys.* **68**, 1649–1664 (1978)
80. Marcus, Y.: Effect of ions on the structure of water: structure making and breaking. *Chem. Rev.* **109**, 1346–1370 (2009)
81. Kestin, J., Sengers, J.V.: New international formulation for the thermodynamic properties of light and heavy water. *J. Phys. Chem. Ref. Data* **15**, 305–320 (1986)

82. Nakahara, M.: Structure, dynamics, and reactions of supercritical water studied by NMR and computer simulation. In: *Water, Steam, and Aqueous Solutions for Electric Power*. Advances in Science and Technology. Proceedings of the 14th International Conference on the Properties of Water and Steam, Japan, Kyoto, 29 August–3 September (2004)
83. Tremaine, P.R., Arcis, H.: Solution calorimetry under hydrothermal conditions. *Rev. Mineral. Geochem.* **76**, 249–263 (2013)
84. Xiao, C.V., Wood, R.H.: Compressible continuum model for ion transport in high-temperature water. *J. Phys. Chem. B* **104**, 918–925 (2000)
85. Balbuena, P.B., Johnston, K.P., Rossky, P.J.: Molecular dynamics simulation of electrolyte solutions in ambient and supercritical water. 1. Ion solvation. *J. Phys. Chem.* **100**, 2706–2715 (1996)
86. Quint, J.R., Wood, R.H.: Thermodynamics of a charged hard sphere in a compressible dielectric fluid. 2. Calculation of the ion–solvent pair correlation function, the excess solvation, the dielectric constant near the ion, and the partial molar volume of the ion in a water-like fluid above the critical point. *J. Phys. Chem.* **89**, 380–384 (1985)
87. Seward, T.M., Driesner, T.: Hydrothermal solution structure: experiments and computer simulations. In: Palmer, D.A., Fernández-Prini, R., Harvey, A.H. (eds.) *Aqueous Systems at Elevated Temperatures and Pressures: Physical Chemistry in Water, Steam and Aqueous Solutions*, Chap. 5, pp. 149–182. Elsevier Academic Press, New York (2004)
88. Driesner, T.: The molecular-scale fundamentals of geothermal fluid thermodynamics. *Rev. Mineral. Geochem.* **76**, 5–33 (2013)
89. Marcus, Y.: Effect of ions on the structure of water: structure making and breaking. *Pure Appl. Chem.* **82**, 1889–1899 (2010)